Development/Plasticity/Repair

The Transcription Factor Sox2 Is Required to Maintain the Cell Type-Specific Properties and Innervation of Type II Vestibular Hair Cells in Adult Mice

Jennifer S. Stone,[1] Rémy Pujol,[1,2] Tot Bui Nguyen,[1] and Brandon C. Cox[3]

[1]Department of Otolaryngology-Head and Neck Surgery and the Virginia Merrill Bloedel Hearing Research Center, University of Washington, Seattle, Washington 98195-7923, [2]Institut National de la Santé et de la Recherche Médicale Unit 1051, Institute of Neuroscience, University of Montpellier, 34000 Montpellier, France, and [3]Departments of Pharmacology and Otolaryngology, Southern Illinois University School of Medicine, Springfield, Illinois 62794-9624

The sense of balance relies on vestibular hair cells, which detect head motions. Mammals have two types of vestibular hair cell, I and II, with unique morphological, molecular, and physiological properties. Furthermore, each hair cell type signals to a unique form of afferent nerve terminal. Little is known about the mechanisms in mature animals that maintain the specific features of each hair cell type or its postsynaptic innervation. We found that deletion of the transcription factor *Sox2* from Type II hair cells in adult mice of both sexes caused many cells in utricles to acquire features unique to Type I hair cells and to lose Type II-specific features. This cellular transdifferentiation, which included changes in nuclear size, chromatin condensation, soma and stereocilium morphology, and marker expression, resulted in a significantly higher proportion of Type I-like hair cells in all epithelial zones. Furthermore, *Sox2* deletion from Type II hair cells triggered non-cell autonomous changes in vestibular afferent neurons; they retracted bouton terminals (normally present on only Type II cells) from transdifferentiating hair cells and replaced them with a calyx terminal (normally present on only Type I cells). These changes were accompanied by significant expansion of the utricle's central zone, called the striola. Our study presents the first example of a transcription factor required to maintain the type-specific hair cell phenotype in adult inner ears. Furthermore, we demonstrate that a single genetic change in Type II hair cells is sufficient to alter the morphology of their postsynaptic partners, the vestibular afferent neurons.

Key words: **afferent nerve terminals; calyx; cell fate; hair cell; Sox2; vestibular**

Significance Statement

The sense of balance relies on two types of sensory cells in the inner ear, Type I and Type II hair cells. These two cell types have unique properties. Furthermore, their postsynaptic partners, the vestibular afferent neurons, have differently shaped terminals on Type I versus Type II hair cells. We show that the transcription factor Sox2 is required to maintain the cell-specific features of Type II hair cells and their postsynaptic terminals in adult mice. This is the first evidence of a molecule that maintains the phenotypes of hair cells and, non-cell autonomously, their postsynaptic partners in mature animals.

Received July 15, 2020; revised Apr. 11, 2021; accepted May 25, 2021.

Author contributions: J.S.S. and B.C.C. designed research; J.S.S., R.P., T.B.N., and B.C.C. performed research; J.S.S., R.P., T.B.N., and B.C.C. analyzed data; J.S.S. and B.C.C. wrote the paper.

This work was funded by National Institutes of Health Grants R01DC013771 (to J.S.S.) and R01DC014441 (to B.C.C.), the Office of the Assistant Secretary of Defense for Health Affairs Grant W81XWH-15-1-0475 (to B.C.C.), and a Virginia Merrill Bloedel Traveling Scholar Award (R.P.). We thank Linda Robinson, Irina Omelchenko, Jialin Shang, and Glen MacDonald from the University of Washington, and Kaley Graves, Michelle Randle, and Chantz Pinder from Southern Illinois University School of Medicine for technical assistance and Connor Finkbeiner and Serena Wisner for their contributions to data analysis. The Core Vision Lab (supported by P30 EY01739) provided technical assistance with preparing TEM sections and access to its JEOL TEM microscope; we acknowledge the help we received from Dale Cunningham and Ed Parker at this facility. We also thank Dr. Suzanne Baker (St. Jude Children's Research Hospital, Memphis, TN) for sharing *Atoh1-CreER^{TM}* mice. Finally, we are grateful to the Hamilton and Mildred Kellogg Charitable Trust for their support for this research.

B.C.C. is a consultant for Turner Scientific, LLC and Otonomy, Inc. All other authors declare no competing financial interests.

Correspondence should be addressed to Brandon C. Cox at bcox@siumed.edu.

https://doi.org/10.1523/JNEUROSCI.1831-20.2021

Introduction

The mammalian nervous system is composed of millions of neurons with diverse properties including cell shape, molecular profiles, and connectivity. Most neurons are formed during development, establishing their unique innervation properties through periods of dynamic growth and differentiation in the embryonic and early postnatal periods. By adulthood, many neurons have established the cell type-specific properties and connectivity that they will maintain throughout life.

These principles are conserved in the vestibular sensory organs of the mammalian inner ear. Each ear has five vestibular epithelia that are composed of sensory hair cells (mechanoreceptors that detect head motions) and non-sensory supporting cells. These epithelia also contain the terminals of vestibular nerve afferents as well as the endings of vestibular efferents. Utricles,

which detect linear head acceleration, have been studied extensively in rodents. Maturation of utricular hair cells and their afferent innervation is complete by the third postnatal week in mice and rats (Ruben, 1967; Sans and Chat, 1982; Burns et al., 2012; McInturff et al., 2018; Wang et al., 2019; Warchol et al., 2019), and at least one vestibular reflex has matured in mice by this time (Faulstich et al., 2004).

Amniotes have two varieties of vestibular hair cells, Type I and Type II, with distinct morphology, physiology, and innervation (for review, see Eatock and Songer, 2011; Burns and Stone, 2017). In rodents, both cell types are distributed across the central and peripheral zones of the organs; in utricles, these zones are referred to as the striola and the extrastriola. Type I hair cells have relatively long and thick stereocilia (the mechanosensory organelles), and their flask-shaped bodies are enveloped by a large afferent nerve terminal called a calyx (Wersall, 1956; Lapeyre et al., 1992; Lysakowski and Goldberg, 1997; Li et al., 2008). Type II hair cells have wider cell bodies and shorter, thinner stereocilia. They possess basolateral cytoplasmic processes (Desai et al., 2005; Pujol et al., 2014), and they synapse on small afferent terminals called boutons. Vestibular afferent neurons also exhibit anatomic diversity. In the chinchilla utricle, most afferents have both calyx and bouton terminals and therefore receive inputs from Type I and Type II hair cells, respectively (Fernández et al., 1990; Goldberg et al., 1990). The remaining neurons have only calyx terminals (limited to the central zone) or only bouton terminals.

The mechanisms that maintain the cell type-specific properties of vestibular hair cells and their postsynaptic neural partners in mature animals are unknown. We hypothesized that the transcription factor Sox2 may reinforce the Type II fate in mature vestibular hair cells because, in adult mice, Sox2 is expressed in Type II, but not Type I, hair cells (Oesterle et al., 2008). Furthermore, *Sox2* is required in early developing murine hair cells for their differentiation to Type II hair cells (Lu et al., 2019). Therefore, we deleted *Sox2* from Type II hair cells in mice at six weeks of age. This single gene deletion caused many Type II hair cells in mature utricles to convert into Type I-like cells and triggered non-cell autonomous changes in vestibular afferent neurons, which retracted their bouton terminals and formed calyx terminals on transdifferentiating hair cells. Transformations occurred in both the striola and the extrastriola.

Our study revealed unexpected plasticity in mature hair cells and primary afferent neurons in the mammalian vestibular periphery. This study is the first to identify a gene required to maintain the type-specific features of hair cells in the adult inner ear. In addition, we show for the first time that the morphology of mature vestibular nerve afferents depends on *Sox2* expression in their presynaptic partner, the hair cell.

Materials and Methods

Mice

Rosa26$^{CAG\text{-}loxP\text{-}stop\text{-}loxP\text{-}tdTomato}$ (*Rosa26*^{tdTomato}; also called Ai14; stock #7914; RRID:IMSR_JAX:007914; Madisen et al., 2010) and *Sox2*$^{loxP/loxP}$ mice (stock #13093; RRID:IMSR_JAX:013093; Shaham et al., 2009) were purchased from The Jackson Laboratory. *Atoh1-CreER*^{TM} mice (RRID:MMRRC_029581-UNC) were a gift from Suzanne Baker at St. Jude Children's Research Hospital (Memphis, TN; Chow et al., 2006). Male and female mice were used in all experiments. When mated, all progeny were on a mixed background dominated by C57Bl/6J. Mice used as neonates were 100% C57Bl/6J and were bred at the University of Washington. Some genotyping was performed by Transnetyx. The *n* value represents the number of mice used in each experiment.

Mice at six weeks of age received two intraperitoneal injections of tamoxifen (9 mg/40 g, Sigma-Aldrich) given with a 20- to 24-h interval between injections. Mice were euthanized by CO_2 gas overdose at various times post-tamoxifen injection. All experiments were performed in accordance with approved animal protocols from the Institutional Animal Care and Use Committees at Southern Illinois University School of Medicine and the University of Washington.

Immunolabeling

Temporal bones were dissected and immersion-fixed in 4% paraformaldehyde [electron microscopy (EM) grade from Polysciences] overnight at room temperature. After fixing, temporal bones were stored in 10 mM PBS (Sigma-Aldrich) at 4°C. Standard immunofluorescence (IF) in whole-mount organs was used to label proteins in hair cells and afferent nerves following previously published protocols (Bucks et al., 2017). Primary antibodies were: goat anti-Sox2 (1:500, Santa Cruz Biotechnology, catalog #sc-17 320, RRID:AB_2286684), rabbit anti-Calb1 (1:200, EMD Millipore, catalog #AB1778, RRID:AB_2068336), rabbit anti-Calb2 (1:500, EMD Millipore, catalog #AB5054; RRID:AB_2068506), mouse anti-Spp1 (1:300, Santa Cruz Biotechnology, catalog #sc-21742, RRID:AB_2194997), goat anti-Anxa4 (1:200, R&D Systems, catalog #AF4146, RRID:AB_2242796), goat anti-OCM (1:200, Santa Cruz Biotechnology, catalog #SC-7446, RRID:AB_2267583), rabbit anti-Tubb3 (1:500, Covance, catalog #PRB-435P, RRID:AB_291637), and mouse anti-βIII tubulin (Tubb3; 1:300, gift from Anthony Frankfurter, University of Virginia). Secondary antibodies were Alexa fluor-conjugated used at 1:300 dilution from Jackson ImmunoResearch. Some samples were counter-labeled with 4',6-diamidino-2-phenylindole (DAPI; 1 µg/ml; Invitrogen) before mounting on slides with Fluorogold (SouthernBiotech) or Prolong Gold (Invitrogen) mounting media.

Confocal microscopy

We used a FV-1000 microscope (Olympus) to obtain high-resolution images of whole-mount utricles. Images were acquired of individual regions and/or the entire utricular sensory epithelium (macula) using either 20× air or 60× oil objectives. Z-series image stacks were attained, starting above the lumen and proceeding to below the supporting cell nuclear layer. Slices were taken at 0.5- to 1.0-µm increments.

Transmission EM (TEM)

Mice were euthanized by CO_2 gas overdose at various times post-tamoxifen injection. The temporal bones were extracted from the skull, and a small hole was made in bone overlying the utricle. Fresh fixative (4% glutaraldehyde in 0.1 M cacodylate buffer; Sigma-Aldrich) was slowly delivered into the hole using a Pasteur pipet. Temporal bones were then placed in fresh 4% glutaraldehyde for 2 h at room temperature followed by storage at 4°C until embedding. Utricles were rinsed in 0.1 M cacodylate buffer, dissected, immersed in 2% osmium tetroxide (Electron Microscopy Sciences) in 0.1 M cacodylate buffer for 1 h, and rinsed in the same buffer again. Utricles were immersed in 1% uranyl acetate (Electron Microscopy Sciences) overnight at 4°C then rinsed in 0.1 M cacodylate buffer. Utricles were plastic-embedded (Eponate #18010, Ted Pella Inc.), and transverse 2-µm sections were taken through the utricle, perpendicular to the anterior-posterior axis, which allowed sampling through both striolar and extrastriolar zones. The striola was identified in sections based on its central location in the section as well as the presence of calyx-only afferents (described in Results), some of which form complex calyces housing more than one hair cell. Every 25–50 µm, we collected a series of ultrathin (80–90 nm) sections on mesh and/or Formvar-coated grids (Ted Pella, Inc). Sections were examined using a JEOL 1230 TEM with an AMT XR80 digital camera at the University of Washington's Vision Core Lab.

For qualitative analyses, we examined utricles from 10 *Sox2* wild-type (WT) mice (four were examined at one month post-tamoxifen, two at five months post-tamoxifen, two at nine months post-tamoxifen, and two were not injected with tamoxifen but were age-matched to the nine month post-tamoxifen mice), and 12 *Sox2* conditional knock-out (CKO) mice (three were examined at two weeks post-tamoxifen, three at

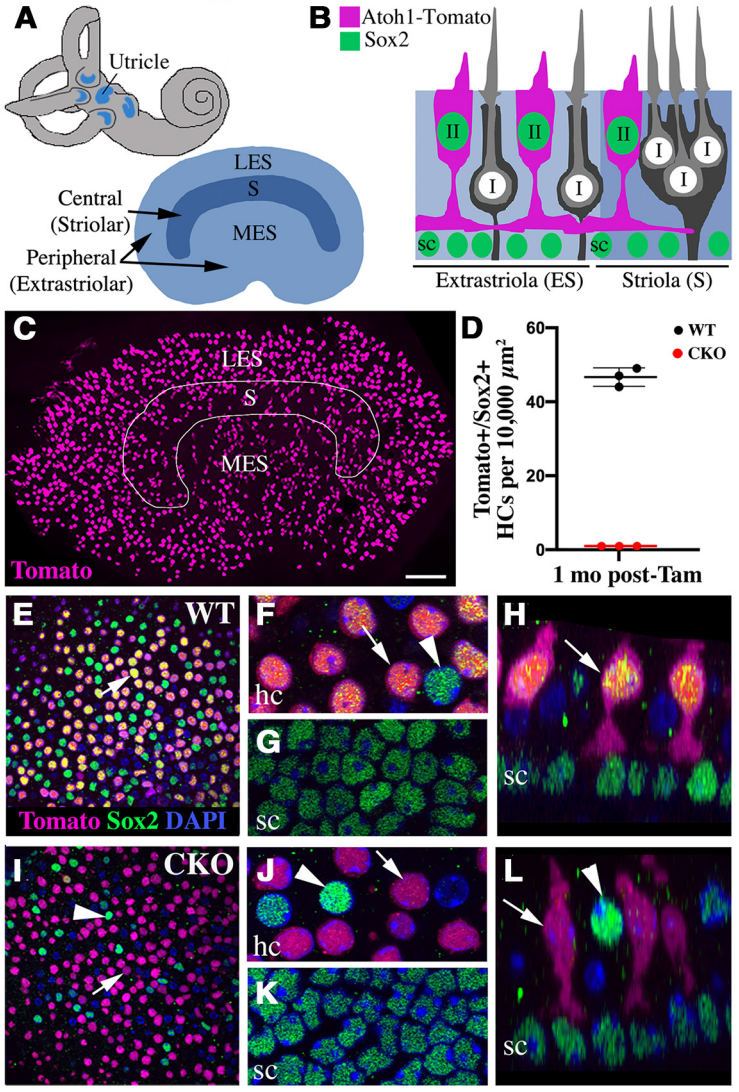

Figure 1. Type II hair cells in *Sox2* CKO mice lost Sox2 protein after tamoxifen treatment. ***A***, upper left, Schematic of the inner ear with vestibular sensory organs in blue. Lower right, Top-down view of the utricle showing its different zones: peripheral (including the LES and MES) and central (including the striola, S). The juxtastriolar zone is small and lies on either side of the striola (data not shown). ***B***, Schematic cross-section of the utricular epithelium; extrastriola is shown on the left, and striola is shown on then right. Type I hair cells (gray), Type II hair cells (magenta), supporting cell nuclei (sc), and afferent calyx terminals (black) are shown. Tomato labeling driven by *Atoh1-CreER*^{T2} is shown in magenta; Sox2 immunolabeling is shown in green. ***C***, Low-magnification confocal image of Tomato-labeled hair cells (magenta) in the utricle of a *Atoh1-CreER*^{TM}*:Rosa26*^{tdTomato} mouse at one week post-tamoxifen. The approximate position of the striola (S) is outlined in white, and the LES and MES are indicated. ***D***, Graph shows density of Tomato-positive hair cells (mean ± SD) that were Sox2-positive in *Sox2* WT and CKO mice at one month post-tamoxifen. $N = 3$ *Sox2* WT mice and 3 *Sox2* CKO mice. ***E–H***, In *Sox2* WT mice at one month post-tamoxifen, Sox2 protein (green) was detected in the nuclei (blue) of Type II hair cells (hc; ***E***, ***F***, ***H***) and supporting cells (sc; ***G***, ***H***). Arrows point to Sox2-positive Type II hair cells that were Tomato-positive (nucleus appears orange when the three channels overlap). Tomato-negative Type II hair cells were also Sox2-positive (arrowhead in ***F***). ***I–L***, In *Sox2* CKO mice, Sox2 protein was lost from Tomato-positive hair cell nuclei (arrows) by one month post-tamoxifen. Tomato-negative hair cells retained Sox2 (arrowheads in ***I***, ***J***, ***L***), as did supporting cells (sc; ***K***, ***L***). All images are top-down views of the utricle except for ***H***, ***L***, which show cross-sections. hc, hair cell layer; sc, supporting cell layer. Scale bar in ***C***: 100 μm (***C***), 30 μm (***E***, ***I***), and 7 μm (***F–H***, ***J–L***).

Table 1. Number of Tomato+ HCI and HCII per utricle

Time post-Tam	*Sox2* WT (mean ± SD)	*Sox2* CKO (mean ± SD)
1 month	1128 ± 114 ($n = 5$)	1110 ± 90 ($n = 9$)
4 months	989 ± 126 ($n = 7$)	1152 ± 240 ($n = 6$)
8 months	988 ± 68 ($n = 3$)	1032 ± 129 ($n = 5$)
ANOVA time effect, *f* value, *p* value	1.442, 0.2529	
ANOVA genotype effect, *f* value, *p* value	1.577, 0.2192	

one month post-tamoxifen, two at five months post-tamoxifen, and four at nine months post-tamoxifen).

Quantitative analysis: confocal micrographs

All of the analyses of confocal images of utricles from *Sox2* WT and CKO mice were performed using Fiji software (Schindelin et al., 2012). For most counts, we tracked "counted cells" using the CellCounter plug-in. For each animal, we examined either the left or right utricle. To avoid bias, genotypes and times post-tamoxifen were masked during analysis. Animal numbers are provided in Results, figure legends, or tables.

For many analyses, we gathered data from the lateral extrastriola (LES), the medial extrastriola (MES), and the striola (Fig. 1*A–C*). The striola was defined by the presence of complex calyces using βIII tubulin immunolabeling of nerve terminals or Calb2 immunolabeling of calyx-only afferent terminals, which are unique to that region (Desai et al., 2005). For Figure 8, the central region (the striola plus a small juxtastriolar region) was defined by Calb1 immunolabeling of afferent nerves and terminals (Prins et al., 2020). The LES and MES zones were readily identified based on the shape of the utricle, gross landmarks such as the medial notch of the sensory epithelium, and the absence of striolar markers (Calb1 or Calb2).

Hair cell counts

We counted Tomato-positive hair cells in 60× images of the entire utricle for *Sox2* WT and CKO mice at one, four, and eight months post-tamoxifen (Table 1). We also counted Tomato-positive Type I and Type II hair cells in specific regions of the utricle (LES, MES, and striola) at one time point, four months post-tamoxifen (Table 2) using criteria defined in the next section. Tomato-negative Type II hair cells were counted in each region as well. We determined the total number of Type II hair cells in the extrastriola (LES plus MES) and the striola (for Tables 4 and 5) by summing Tomato-positive and Tomato-negative Type II hair cells. We estimated the number of Type I hair cells in these regions by multiplying the striolar Type II hair cell number by 1.47 and the extrastriolar Type II hair cell number by 1.19; these numbers are ratios of Type I:II hair cells in mice, obtained from Desai et al. (2005). By summing regional counts, we estimated that each utricle has 3041 hair cells (Type I and Type II that are either Tomato-negative or Tomato-positive). These estimates were a little smaller than those of Desai et al. (2005) presumably because we subdivided the utricle into LES, MES, and striolar regions and excluded cells from counts that were on the borders of these regions.

Identifying Type I and Type II hair cells

Assignment of a cell as Type I or Type II was required for several analyses. Most of these analyses were performed in the extrastriola, where classification as Type I or Type II was easiest because the nuclei of the

Table 2. Tomato+ HCs

	Number of Tom+ HCI and HCII per region in *Sox2* WT			Number of Tomato+ HCII in *Sox2* WT	
Region	Time post-Tam	Mean ± SD	% of total utricle	*Sox2* WT 4 months post-Tam	
LES	4 months ($n = 3$)	577 ± 56	61%	Number of Tom+ HCII per Ut	870 ± 90
MES	4 months ($n = 3$)	208 ± 31	22%	% of Tom+ HCs that were HCII	92
Striola	4 months ($n = 3$)	163 ± 40	17%		
Whole utricle	4 months ($n = 3$)	949 ± 101	100%		

two cell types are separated into distinct layers. As described in Figs. 1*B*, 2*E* and in Pujol et al. (2014), Type II nuclei are located in a near-monolayer closest to the lumen, while Type I nuclei are positioned in a near-monolayer between the Type II nuclei and the supporting cell nuclei, which are most basal. DAPI labeling enabled localization of the nuclei in confocal Z-series images. We always applied additional criteria beside lamination to classify cells as Type I or Type II. Type I hair cells had a long, skinny neck and a rounded basolateral surface lacking cytoplasmic processes, which were readily detected in Tomato-positive and/or myosin VIIa-labeled cells. Type I cells also had an afferent calyx that surrounded the cell body at the level of the nucleus, as demonstrated by antibodies to βIII tubulin (used in most of our preparations). Type II hair cells had a thick neck and one or more basolateral processes, and they lacked a calyx. Each hair cell had to possess several cell type-specific features, including nuclear location, morphologic features, and presence/absence of calyx, to fit into one category or the other. In most cases, hair cell cells met all criteria. In *Sox2* CKO mice, however, it was difficult to rely on nuclear lamina for cell typing because nuclear layers were less defined in some places, particularly at later survival times post-tamoxifen. In these cases, we relied more heavily on the other cell-typing criteria.

Sox2 immunolabeling

We measured the density of Tomato-positive hair cells that were either Sox2-positive or Sox2-negative in utricles that were immunolabeled for Sox2. We sampled 17% – 34% of the sensory epithelium, including the LES, MES, and striola.

Calb2 IF intensity and nuclear size

We measured nuclear Calb2 IF intensity and nuclear area in the same Tomato-positive cells in 60× confocal microscope images (1-µm steps), sampling 19–25% of each macula in the LES and MES regions. We analyzed all Tomato-positive cells in each field, classifying them as Type I or Type II as described earlier in this section.

For each cell, we identified the slice that bisected each nucleus at its largest area. Then, using the drawing tool in Fiji, we circled the nucleus and measured (1) the Calb2 intensity of the nucleus (mean gray value) at that position and (2) the area of the nucleus. To normalize Calb2 labeling for each cell type, we subtracted background intensity measured in the supporting cell cytoplasm (which appeared Calb2-negative) in each corresponding layer. In Figure 2*D*, data are presented as the mean cellular value for each animal in a group. In Figure 2*C*, we present data for all cells from a representative mouse in each group; this animal had a mean Calb2 IF level close to the group mean.

Spp1, Anxa4, and Ocm immunolabeling. We scored all Tomato-positive hair cells per utricle (extrastriola only) as positive or negative for Spp1 in 60× images. Cells were considered Spp1-positive if they had strong labeling in the apical (neck) region. We did the same analysis for Anxa4; Tomato-positive cells were scored as Anxa4-positive if they had strong labeling near the plasma membrane at the level of the nucleus. We scored all Tomato-positive hair cells in the striola as positive or negative for Ocm in 60× images. Cells were considered Ocm-positive if they had strong labeling in their cytoplasm and nucleus.

Calyx analysis

To determine how many Tomato-positive hair cells in the extrastriola had a calyx, utricles were immunolabeled for Tubb3, which is abundant in neurites and neural terminals. In 60× images, we counted all Tomato-positive hair cells in the LES and MES of each utricle that had a calyx, defined as continuous Tubb3 label around its entire cell body at the level of the nucleus (see Fig. 5*A2*,*B2*). In some cells, this included full extension of Tubb3 label along the cell's neck. We were unable to reliably differentiate partial from full calyces using Tubb3 labeling; there was too much noise from the bouton labeling, making it hard to distinguish closely arranged boutons from a partial calyx.

To count Tomato-positive hair cells in the striola that had a calyx, utricles were immunolabeled for Calb2, which is abundant in calyx-only fibers but is not detected in dimorphic afferents in this region. In 60× images, we counted all Tomato-positive hair cells in the striola of each utricle that had a partial calyx (Calb2 label contacting between 10% and 70% of the cell body) or a full calyx (continuous Calb2 labeling around greater than ~90% of the cell body). It is important to note that we could easily distinguish the cytoplasmic Calb2 labeling in Type II hair cells from the calyceal Calb2 labeling because the calyx was much more strongly labeled (Fig. 6).

Maps of converting/converted cells

We plotted extrastriolar Tomato-positive hair cells with Type I-like morphology and striolar Tomato-positive hair cells with a Calb2-labeled calyx from one representative utricle from a *Sox2* WT and a CKO mouse at four months post-tamoxifen. We took screenshots from CellCounter (Fiji) of every part of the utricle (60× montages) and imported them to Adobe Photoshop. In a new layer, we generated dots for each cell and then created the outline of the sensory epithelium.

Striolar area

We estimated the area (µm^2) of the central zone (striola plus juxtastriola) in utricles labeled with antibodies to Calb1, which labels afferent fibers and calyces in the central region (Prins et al., 2020). Using Fiji, we drew a line around the portion of the macula that contained Calb1-positive calyces and measured the area.

Quantitative analysis: electron micrographs

We measured the width of individual stereocilia in TEM images from the LES and MES regions using Fiji in *Sox2* WT and CKO mice at one month and five to nine months post-tamoxifen. For each hair cell, we averaged widths from three stereocilia. Not all stereocilia from a bundle had the same diameter, and the diameter of one single stereocilium varied along its length (thicker at the apex), so we measured the three thickest stereocilia present in each image at the point of its thickest diameter.

Statistics

GraphPad Prism version 7 was used for all statistical analyses. The test applied to each set of data are described in Results. *Post hoc* multicomparisons analyses for one-way and two-way ANOVAs were performed using a Dunnett's or Tukey's test, respectively. All data are presented as mean and standard deviation. Differences were considered to be significant if $p \leq 0.05$.

Results

Type II hair cells with *Sox2* deletion lost Type II molecular markers and gained Type I markers

This study was conducted in young adult mice starting at 6 weeks of age. We studied the utricle, which is one of five vestibular organs in each inner ear (Fig. 1*A*) and is specialized for

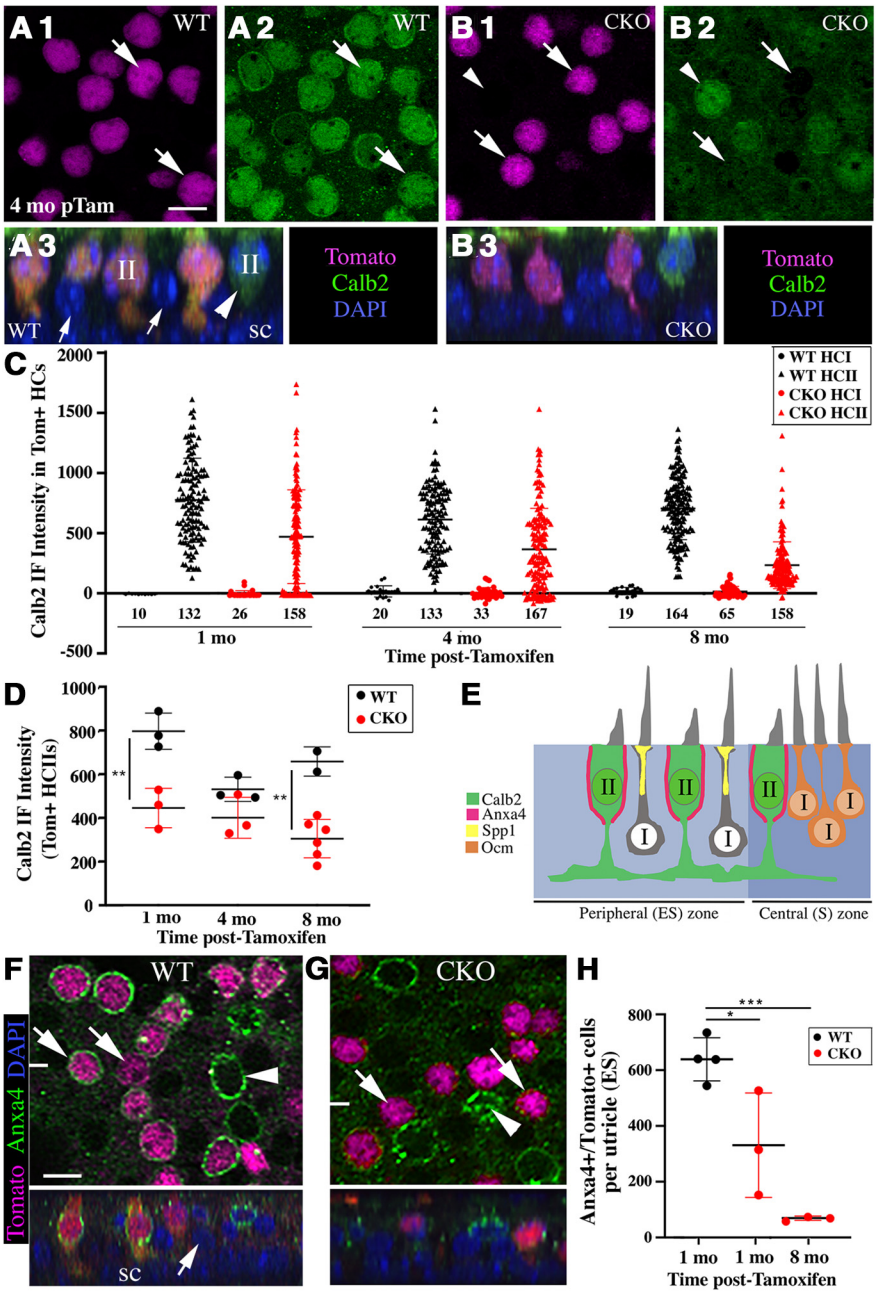

Figure 2. Type II hair cells lost immunoreactivity for two Type II-specific markers following *Sox2* deletion. ***A1***, ***A2***, Top-down views of the extrastriolar epithelium showing the same field of a *Sox2* WT mouse at four months post-tamoxifen. In ***A1***, ***A2***, arrows point to Tomato-positive cells (magenta) that are immunoreactive for Calb2 (green). **A3.** Vertical slice from another region showing Calb2 labeling in Tomato-positive Type II hair cells (II) and a Tomato-negative Type II hair cell (arrowhead). Supporting cells (sc) and Type I hair cells (arrows) were Tomato-negative. ***B1***, ***B2***, Top-down views of the extrastriolar epithelium showing the same field of a *Sox2* CKO mouse at four months post-tamoxifen. Tomato-positive hair cells (arrows) appeared Calb2-negative; Tomato-negative hair cells (arrowheads) retained Calb2 immunoreactivity, as expected. ***B3***, Tomato-positive cells with very weak Calb2 immunolabeling. ***C***, Cell population data showing distributions of Calb2 IF intensity in Type I hair cells (HCI) and Type II hair cells (HCII) from one representative mouse of each group (WT or *Sox2* CKO mice at one, four, or eight months post-DT). Each dot represents one cell. Black bar shows the average while red bar shows ± 1 SD. ***D***, Graph shows mean $\pm$ 1 SD for Calb2 IF intensity in each group. Each dot represents the mean intensity level for all cells analyzed in a given animal; $n = 3$ mice per group except for eight months WT (two mice) and eight months CKO (six mice); $^{**}p < 0.01$. ***E***, Illustration of different cell type-specific markers in peripheral (extrastriolar; ES) and central (striolar; S) regions of the utricle. ***F***, upper panel, Top-down views of the extrastriolar epithelium from a *Sox2* WT mouse at one month post-tamoxifen. Tomato-positive (magenta) hair cells (arrows) were immunoreactive for Anxa4 (green), as were Tomato-negative Type II hair cells (arrowhead). Lower panel shows a vertical slice through the area indicated by the horizontal white line (left side, half-way down). Tomato-positive hair cells were Anxa4-positive while supporting cells (sc) and Type I hair cells (arrow) were not. ***G***, Images, showing *Sox2* CKO mice at eight months post-tamoxifen, are the same format as in ***F***. In *Sox2* CKO mice, Tomato-positive hair cells (arrows) had lost Anxa4 labeling; Tomato-negative hair cells (arrowheads) retained Anxa4 immunoreactivity, as expected. ***H***, Graph shows mean number (± 1 SD) of Tomato-positive hair cells that were Anxa4-positive. Each dot represents the average for one animal; $n = 4$ for the *Sox2* WT at one month post-Tam and $n = 3$ mice for the two *Sox2* CKO groups; $^{*}p < 0.05$, $^{***}p < 0.001$. Scale bar in ***A1***: 6 μm (***A1–B3***). Scale bar in ***F*** (lower left): 6 μm (***F***, ***G***).

detecting linear head motions. In mice, the utricle is a disk-shaped organ whose sensory epithelium (macula) has two zones: the central zone, which is also called the striola, and the peripheral zone, which is further subdivided into the LES and MES. Both Type I and Type II hair cells are distributed throughout these zones (Fig. 1*B*; Desai et al., 2005; Kirkegaard and Nyengaard, 2005; Li et al., 2008; Pujol et al., 2014). Studies in chinchilla showed that most vestibular afferents innervating hair cells are dimorphic: they have both calyx and bouton terminals (Fernández et al., 1990; Goldberg et al., 1990). Dimorphic afferents are distributed throughout all zones of the utricle; the remaining afferent neurons are either calyx-only (confined to the striola) or bouton-only (confined to the extrastriola).

To test the hypothesis that Sox2 is required to maintain the Type II hair cell phenotype, we deleted *Sox2* from Type II hair cells using $Sox2^{loxP/loxP}$ mice, which have *loxP* sites flanking the single *Sox2* exon (Shaham et al., 2009). To target Type II hair cells, we employed transgenic $Atoh1\text{-}CreER^{TM}$ mice (Chow et al., 2006), which in adult utricles have tamoxifen-inducible Cre activity primarily in Type II hair-cells (Bucks et al., 2017); details are described below. We generated $Atoh1\text{-}CreER^{TM}$:$Rosa26^{tdTomato}$:$Sox2^{loxP/loxP}$ (*Sox2* CKO) mice, in which tamoxifen drives expression of the fluorescent protein tdTomato (Tomato) for fate-mapping cells with *Sox2* deletion. $Atoh1\text{-}CreER^{TM}$:$Rosa26^{Tomato}$:$Sox2^{+/+}$ littermates (*Sox2* WT) served as negative controls in which Tomato was expressed in Type II hair cells and *Sox2* remained intact following tamoxifen injection.

First, we characterized Tomato labeling in *Sox2* WT mice. At four months after tamoxifen injection at six weeks of age, there were 989 ± 126 (mean ± SD) Tomato-positive hair cells per utricle (Fig. 1*C*). Numbers were similar at one, four, and eight months post-tamoxifen (Table 1), which was expected because there is little death of hair cells in adult mouse utricles (Bucks et al., 2017). As described previously (Bucks et al., 2017), Tomato-positive supporting cells were rare (1–3 cells per utricle), and Tomato expression was absent from vestibular neurons and glia.

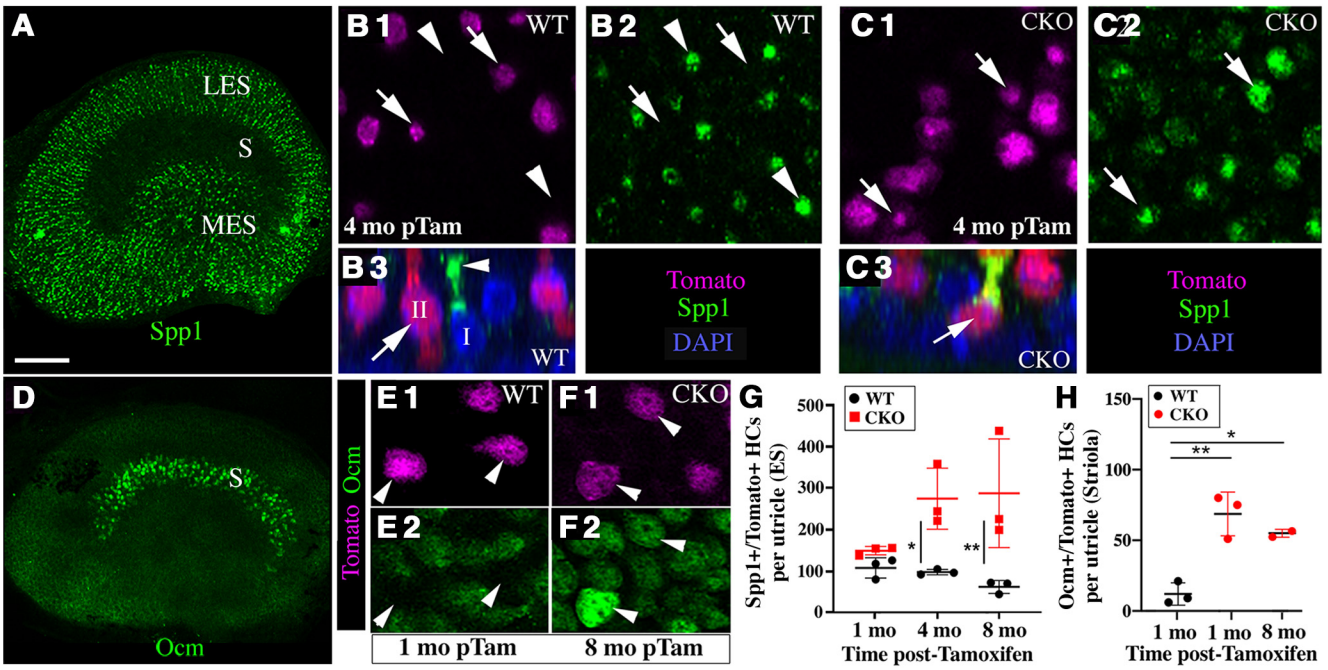

Figure 3. Type II hair cells gained immunoreactivity for two Type I-specific markers following *Sox2* deletion. ***A***, Low-magnification top-down view of Spp1 immunolabeling in adult utricle. S, striola; LES, lateral extrastriola; MES, medial extrastriola. ***B1***, ***B2***, Top-down views of Spp1-labeled extrastriolar epithelium showing the same field of a *Sox2* WT mouse at four months post-tamoxifen. In ***B1***, ***B2***, arrows point to Tomato-positive cells (magenta) that lack Spp1 immunolabeling (green). Arrowheads indicate Tomato-negative cells that are Spp1-positive. ***B3***, Vertical slice from another region showing lack of Spp1 labeling in Tomato-positive Type II hair cells (II; arrow) and Spp1 labeling in the neck of a Tomato-negative Type I hair cell (I; arrowhead). ***C1***, ***C2***, Top-down views of Spp1-labeled extrastriolar epithelium showing the same field of a *Sox2* CKO mouse at four months post-tamoxifen. Tomato-positive hair cells (magenta, arrow) were Spp1-positive. ***C3***, Spp1-positive/Tomato-positive hair cell (arrow) shown in a slice. ***D***, Low-magnification top-down view of Ocm immunolabeling in adult utricle. S, striola. ***E1***, ***E2***, Top-down views of the striolar epithelium showing the same field of a *Sox2* WT mouse at one month post-tamoxifen. Arrowheads point to the same Tomato-positive cells (magenta) that lack Ocm immunolabeling (green). ***F1***, ***F2***, Top-down views of the striolar epithelium showing the same field of a *Sox2* CKO mouse at eight months post-tamoxifen. Arrowheads point to the same Tomato-positive cells (magenta) that are Ocm-positive (green). ***G***, Graph shows number of extrastriolar Tomato-labeled hair cells per utricle that were Spp1-immunoreactive in *Sox2* WT and CKO mice at various times post-tamoxifen**.** ***H***, Graph shows number of striolar Tomato-labeled hair cells per utricle that were Ocm-immunoreactive in *Sox2* WT mice at one month post-tamoxifen and in *Sox2* CKO mice at one and eight months post-tamoxifen. For both graphs, data are expressed as mean ± SD. Each point is the average number for each mouse in the group; $*p < 0.05$, $**p < 0.01$. Scale bar in ***A***: 150 μm (***A***, ***D***), 12 μm (***B1–C3***), and 10 μm (***E1–F2***).

Labeled hair cells were fairly evenly distributed through all zones. 61% of labeled cells were in the LES, 22% in the MES, and 17% in the striola (Fig. 1*C*; Table 2, left side), these proportions reflect the relative areas of each zone. Most labeled hair cells (92%) were Type II (Table 2, right side). A large proportion of Type II hair cells in each region were Tomato-positive: 60% in the LES, 72% in the MES, and 60% in the striola. Less than 10 Tomato-positive hair cells and supporting cells per utricle were present in *Sox2* WT mice when no tamoxifen was given (Bucks et al., 2017).

To verify the loss of Sox2 protein from Type II hair cells of *Sox2* CKO mice, we immunolabeled utricles at one month post-tamoxifen (Fig. 1*E–L*). *Sox2* WT mice had significantly higher density of Tomato-positive/Sox2-positive hair cells than *Sox2* CKO mice (unpaired Student's *t* test $p < 0.0001$, $t = 31.43$, $df = 4$; Fig. 1*D*). On average, 98% of Tomato-positive Type II hair cells in *Sox2* WT mice were Sox2-positive (Fig. 1*E–H*) compared with 2% in *Sox2* CKO (Fig. 1*I–L*). Tomato-negative Type II hair cells retained Sox2 labeling in *Sox2* CKO mice (Fig. 1*J*), as did supporting cells, which also normally express Sox2 (compare Fig. 1*G*,*H* and *K*,*L*). This was expected because Tomato-negative cells should lack CreER activity. We observed a similar loss of Sox2 at two weeks post-tamoxifen (data not shown), but this was not quantified.

We found no difference in numbers of Tomato-positive hair cells per utricle among *Sox2* WT and CKO mice at one, four, and eight months times post-tamoxifen (Table 1). Two-way ANOVA confirmed no effect of either genotype ($p = 0.2192$, $f = 1.58$) or time post-tamoxifen ($p = 0.2529$, $f = 1.44$). This finding strongly suggested that *Sox2* deletion from Type II hair cells did not cause them to die.

To test *Sox2*'s requirement for maintaining the Type II hair cell phenotype in adult mice, we gave tamoxifen to six-week-old *Sox2* WT and CKO mice and examined hair cells at three times post-tamoxifen: two weeks, one month, four to five months, and eight to nine months. We assessed molecular, morphologic, and ultrastructural criteria that are specific to the Type I or Type II hair cell phenotype in Tomato-positive hair cells.

First, we looked at expression of the calcium-binding protein calretinin (Calb2), which is a selective marker for Type II hair cells (Desai et al., 2005; Pujol et al., 2014; Fig. 2*E*). In *Sox2* WT mice, antibodies to Calb2 labeled the cytoplasm and nucleus of 96 ± 0% of extrastriolar Type II hair cells (four months post-tamoxifen is shown; Fig. 2*A1–A3*) and 97 ± 0% of striolar Type II hair cells (Fig. 6*C*). Type I hair cells and supporting cells appeared Calb2-negative (Fig. 2*A3*). Calb2 IF was reduced in *Sox2* CKO mice relative to *Sox2* WTs (four months post-tamoxifen is shown; compare Figs. 2*B1–B3* and 2*A1–A3*, 2*D*).

We measured Calb2 IF intensity in Tomato-positive cells in *Sox2* WT and CKO mice. We sampled 19–25% of the extrastriolar epithelium (LES and MES), classifying each Tomato-positive cell as Type I or Type II and measuring Calb2 intensity in each cell, as described in Materials and Methods. Figure 2*C* shows cell population data from one representative animal at each time point. Each data point represents an individual hair cell, with cell

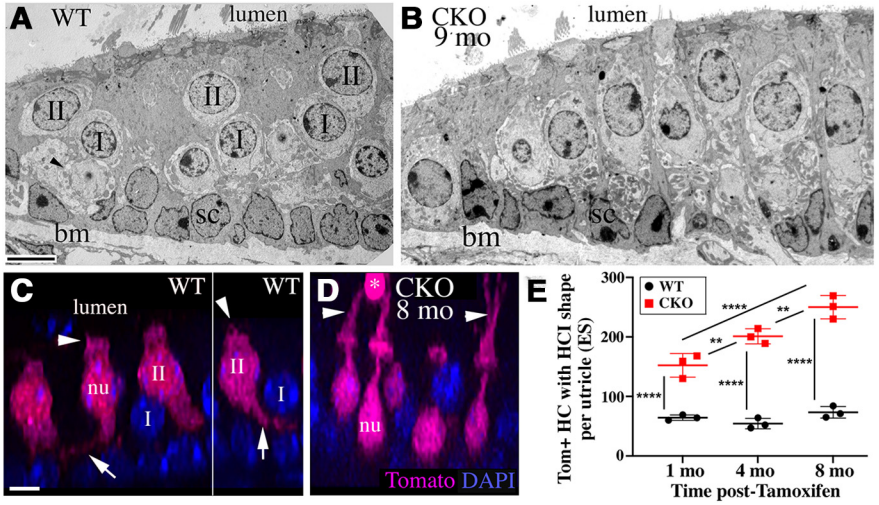

Figure 4. Changes in Type II hair cell position and shape following Sox2 deletion. All images were taken from the same approximate region in the LES. ***A***, ***B***, Low-magnification TEM images from a *Sox2* WT mouse (***A***) and a *Sox2* CKO mouse (***B***), both at nine months post-tamoxifen. Note that the WT epithelium has two hair cell layers (Type II near the lumen, and Type I more deeply located), while this lamination was less clear in some regions after *Sox2* CKO. I, Type I hair cell; II, Type II hair cell; bm, basement membrane; sc, supporting cell. Scale bar in ***A***: 7 μm (also applies to ***B***). ***C***, ***D***, Confocal vertical re-slices of Tomato-positive hair cells a *Sox2* WT mouse (***C***) and a *Sox2* CKO mouse (***D***). In WTs, most Tomato-positive hair cells had Type II-like morphology: a thick cell body, short stereocilia (arrowheads), nuclei (nu) located close to the lumen, and basolateral processes (arrows). In *Sox2* CKO mice, more Tomato-positive hair cells were Type I-like; they had flask-shaped cell bodies, long stereocilia (arrowheads), nuclei (nu) located deeper than the Type II hair cell nuclei, and no basolateral processes. Asterisk shows a cytoplasmic bleb from a hair bundle. Note that panel ***C*** contains two separate non-continuous panels separated by a thin line, showing four exemplary Tomato-positive Type II hair cells from a WT mouse. Scale bar in ***C***: 6 μm (also applies to ***D***). ***E***, Graph shows number of extrastriolar Tomato-positive hair cells per utricle that had Type I-like morphology for *Sox2* WT and CKO mice at various times post-tamoxifen. Data are expressed as mean ± 1 SD. Each point is the average number for each mouse in the group; for all groups, $n = 3$ mice; $^{**}p < 0.01$, $^{****}p < 0.0001$.

numbers listed below each column on the *x*-axis. As expected for *Sox2* WT mice, the average Calb2 intensity in Type I hair cells was much lower than Type II hair cells at all times. Interestingly, WT Type II hair cells had a large range of Calb2 intensities. In *Sox2* CKO mice, there was a reduction in average Calb2 intensity in Type II hair cells at all times post-tamoxifen and an increase in numbers of Tomato-positive Type I hair cells.

We computed the average Calb2 intensity of Type II hair cells for each in a group (Fig. 2*D*). Two-way ANOVA of group data in Figure 2*D* showed a significant effect of genotype ($p < 0.0001$, $f = 50.48$) and time post-tamoxifen ($p = 0.0109$, $f = 6.350$), indicating that Calb2 IF had decreased in *Sox2* CKO mice relative to WT by one month post-tamoxifen and did not decrease further over time. Although we only measured IF intensity in extrastriolar hair cells, we noted a similar loss of Calb2 IF in striolar hair cells (compare Fig. 6*C* and *D*).

We investigated whether extrastriolar Type II hair cells lost a second marker, annexin A4 (Anxa4), after *Sox2* deletion. Anxa4 is only expressed in Type II hair cells (McInturff et al., 2018) and is localized to the cell's periphery (Fig. 2*E*), appearing as ring around the cell in top-down views of *Sox2* WT utricles at one month post-tamoxifen (Fig. 2*F*). After *Sox2* CKO, numbers of Anxa4-positive hair cells decreased significantly relative to WT controls ($p = 0.0009$, $f = 22.34$, by one-way ANOVA; Fig. 2*F–H*). This reduction was significant at one month post-tamoxifen and became significantly larger at eight months post-tamoxifen. These observations provided further evidence that mature Type II hair cells lost cell-specific properties following *Sox2* deletion.

Next, we tested whether Type II hair cells acquired Type I-specific properties after *Sox2* CKO. First, we labeled utricles with antibodies to secreted phosphoprotein 1 (Spp1; also called osteopontin). Spp1 is a selective marker for Type I hair cells in the extrastriola (McInturff et al., 2018; Fig. 2*E*). In the utricles of mature mice, Spp1 is expressed in type I hair cells but not type II hair cells (McInturff et al., 2018)(Fig. 2*E*). In *Sox2* WT mice, we found most Spp1 labeling to be extrastriolar (Fig. 3*A*). As expected, type II hair cells (either Tomato-positive or negative) were Spp1-negative, and type I hair cells were Spp1-positive (Fig. 3*B1–B3*). After *Sox2* CKO, numbers of Tomato-positive hair cells that were Spp1-positive per utricle increased significantly (Fig. 3*C1–C3*;*G*). Two-way ANOVA showed an effect of genotype ($p = 0.0003$, $f = 25.10$) but no effect of time post-tamoxifen ($p = 0.2795$, $f = 1.42$). Numbers did not increase in *Sox2* CKO mice until four months post-tamoxifen, and after that time they did not increase significantly (Fig. 3*G*).

We also tested whether Type II hair cells in the striola gained a Type I-specific marker after *Sox2* CKO by labeling utricles with antibodies to oncomodulin (Ocm), which is expressed in the cytoplasm and nucleus of striolar Type I hair cells (Simmons et al., 2010; see Fig. 2*E*,3*D*). In *Sox2* WT mice at one month post-tamoxifen, very few Tomato-positive hair cells (Type II) were Ocm-positive (Fig. 3*E1*, *E2*, *H*). After *Sox2* CKO, numbers of Tomato-positive cells that were Ocm-positive were significantly higher (Fig. 3*F1*, *F2*, *H*) than WT mice at both of the times we examined ($p = 0.0037$, $f = 20.9$, by one-way ANOVA).

These analyses showed that *Sox2* deletion from Type II hair cells caused them to lose Type II-selective markers (Calb2 and Anxa4) and to gain Type I-selective markers Spp1 in the extrastriola and Ocm in the striola.

Type II hair cells adopted Type I morphology following *Sox2* deletion

Next, we explored whether *Sox2* deletion from Type II hair cells caused them to acquire Type I-like morphology. For this analysis, we focused on the extrastriola (MES and LES), where the cell nuclei are clearly organized into three layers and the shapes of the two hair cell types are consistently distinct from each other (Figs. 1*B*, 2*E*). The cellular lamination in the extrastriolar epithelium is evident in a low-magnification transmission electron micrograph (TEM) of a *Sox2* WT mouse at nine months post-tamoxifen (Fig. 4*A*). By contrast, after *Sox2* CKO, the epithelial lamination was lost in some places (Fig. 4*B*), presumably because many Type II nuclei had migrated to a more basal (Type I-appropriate) position as they underwent transdifferentiation.

We used confocal microscopy to analyze the shape of Tomato-positive hair cells and classify them as either Type I or Type II (described in Materials and Methods). In *Sox2* WT mice, as anticipated based on marker labeling, most Tomato-positive hair cells were Type II-like in cell shape, and they did not change their morphology over time post-tamoxifen (Fig. 4*C*,*E*). After *Sox2* CKO, however, the numbers of Tomato-positive hair cells

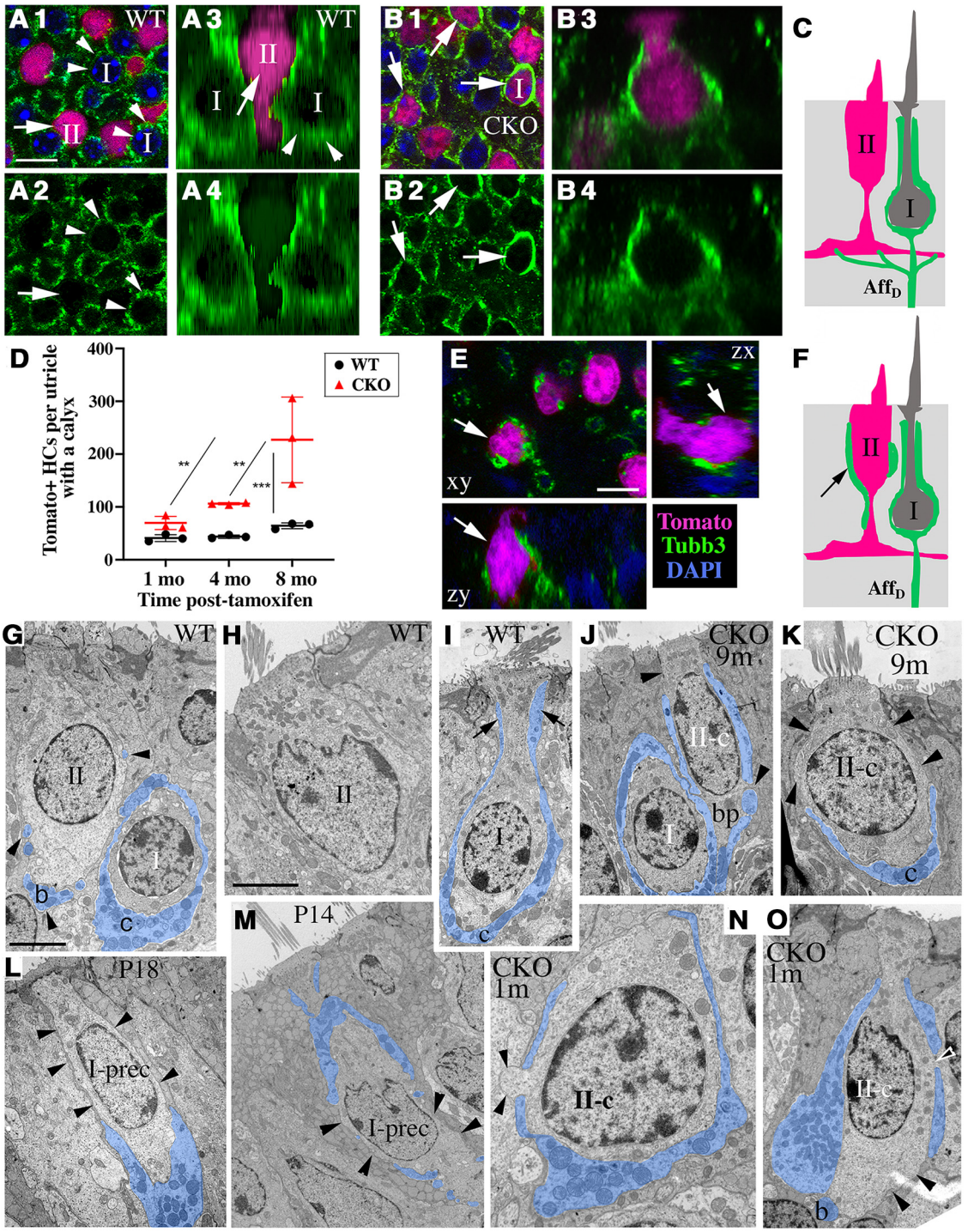

Figure 5. Extrastriolar Type II hair cells gained a full or partial calyx afferent following *Sox2* deletion. ***A1***, ***A3***, In *Sox2* WT mice at four months post-tamoxifen, Tomato-positive hair cells (magenta, arrows) were Type II-like and lacked a calyx (labeled with antibodies to Tubb3, green). By contrast, Type I hair cells (arrowheads), which were Tomato-negative, had a calyx. ***A2***, ***A4***, Same fields as ***A1***, ***A3*** but just the Tubb3 channel. ***B1***, ***B3***, In *Sox2* CKO mice at four months post-tamoxifen, some Tomato-positive hair cells (magenta, arrows) were Type I-like, with most of their cell body enwrapped by a calyx. ***B2***, ***B4***, Same fields as ***B1***, ***B3*** but just the Tubb3 channel. ***C***, Depiction of the appearance of cells in *Sox2* WT mice, with dimorphic afferent nerve (Aff$_D$, green) surrounding a Type I hair cell as a calyx and contacting a Tomato-positive Type II hair cell as bouton terminals. ***D***, Graph shows the number of extrastriolar Tomato-labeled hair cells per utricle (mean ± SD) with a calyx in *Sox2* WT and CKO mice at different times post-tamoxifen. Each point is the average number for each mouse in the group. $N = 3$ mice for all groups; $^{**}p < 0.01$, $^{***}p < 0.001$. ***E***, Image from a *Sox2* CKO mouse at four months post-tamoxifen showing a Tomato-positive cell with a partial calyx (arrow). xy, top-down view, while xz and yz are slices of the same field in each plane. ***F***, Drawing of Tomato-positive hair cell partially enveloped by calyx nerve afferent (green), similar to what is shown for a *Sox2* CKO mouse in panel ***E***. ***G–O***, TEM images of cells from the extrastriolar region. All afferent nerve terminals are pseudo-colored in blue. ***G–I***, Exemplary Type I and Type II hair cells from *Sox2* WT mice. Calyx afferents (c) fully enwrap the Type I hair cell body, up to the neck (arrows in ***I***). Bouton afferents (b and arrowheads in ***G***) only contact Type II hair cells. ***J***, ***K***, ***N***, ***O***, Examples of presumed converting Type II hair cells (II-c) with a partial calyx in *Sox2* CKO mice at one or nine months (m) post-tamoxifen. Arrowheads point to places where the calyx is lacking; in one case (***N***), the hair cell cytoplasm bulges between the two pieces of calyx material. ***L***, ***M***, Examples of presumed Type I hair cell precursors (I-prec) with a partial calyx in developing mouse utricles at P18 (***L***) and P14 (***M***). Arrowheads point to places where the calyx is lacking. I, Type I hair cell; II, Type II hair cell; sc, supporting cell; bm, basal membrane; bp, basolateral process. Scale bar in ***A1***: 6 μm (*A1–B4*); in ***E***: 6 μm; in ***G***: 5 μm (***G***, ***I***, ***J***, ***L***, ***M***, ***O***) and 1 μm (***N***); and in ***H***: 3 μm (***H***, ***K***).

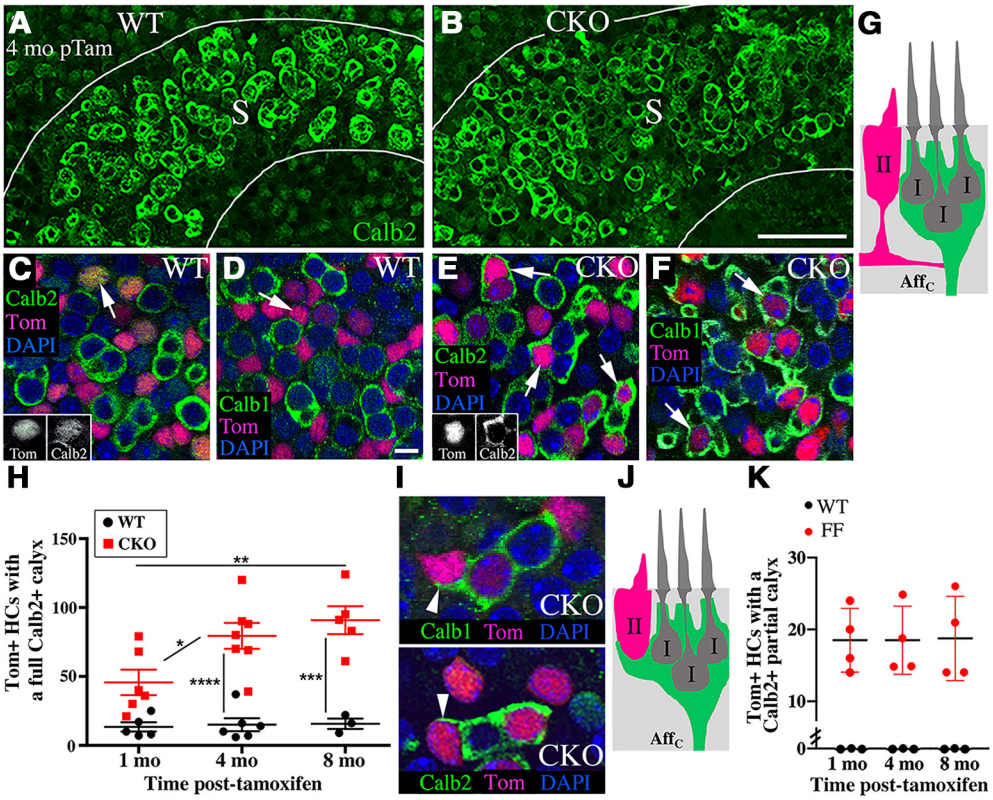

Figure 6. Type II hair cells in the striola joined calyx-only afferents following *Sox2* deletion: Evidence with confocal microscopy. ***A***, ***B***, Calb2 (green) labeling of calyx-only afferents in the striola from *Sox2* WT and CKO mice at four months post-tamoxifen. Calb2 is highly expressed in calyx-only afferents, which are confined to the striola (S; outlined in white). ***C–F***, Images from the striola showing calyx-only afferents labeled for Calb2 (***C***, ***E***) or Calb1 (***D***, ***F***) from *Sox2* WT or CKO utricles at four months post-tamoxifen. Arrows point to Tomato-positive hair cells (magenta) that were surrounded by a Calb2 or a Calb1-labeled calyx in mice with *Sox2* CKO (***D***, ***F***) but not in *Sox2* WT (***C***, ***E***) mice. Insets in ***C***, ***E*** show Tomato and Calb2 nuclear labeling in separate channels for the cells indicated by arrows. ***G***, Depiction of the appearance of cells in *Sox2* WT mice with a calyx-only afferent nerve (Aff$_C$, green) surrounding Type I hair cells. This example is a complex calyx afferent. The tomato-positive Type II hair cell is not contacted by the calyx-only afferent. ***H***, Graph shows the number of Tomato-positive (Tom+) striolar hair cells per utricle (mean ± SD) that were fully or mostly wrapped by a Calb2-labeled calyx. Each point is the average number for each mouse in the group. For *Sox2* WT, $n = 5$ mice at one month, 6 mice at four months, and 3 mice at eight months post-tamoxifen. For *Sox2* CKO, $n = 6$ mice at one month, 7 mice at four months, and 5 mice at eight months post-tamoxifen; $^{*}p < 0.05$, $^{**}p < 0.01$, $^{***}p < 0.0001$, $^{****}p < 0.0001$. ***I***, *Sox2* CKO utricles labeled with antibodies to Calb1 (top) or Calb2 (bottom), showing complex calyces extending neurites (arrowheads) to enwrap nearby Tomato-positive hair cells. ***J***, Drawing of Tomato-positive hair cell partially enveloped by calyx nerve afferent (green), similar to what is shown for *Sox2* CKO mice in panel ***I***. ***K***, Graph shows the number of Tomato-positive (Tom+) striolar hair cells per utricle (mean ± SD) that were partially wrapped by a Calb2-labeled calyx. Each point is the average number for each mouse in the group. For *Sox2* WT, $n = 4$ mice at each time post-tamoxifen; for *Sox2* CKO, $n = 3$ mice at each time post-tamoxifen. Scale bar in ***B***: 25 μm (***A***, ***B***); and in ***D***: 4 μm (***C–F***) and 6 μm (***I***).

with a Type I morphology increased significantly (Fig. 4*D*,*E*). Two-way ANOVA showed effects of genotype ($p < 0.0001$, $f = 410.30$) and time post-tamoxifen ($p < 0.0001$, $f = 24.75$), with a significant difference in Type I-like hair cells between *Sox2* WT and CKO mice as early as one month post-tamoxifen and with significant differences between *Sox2* CKO mice at all times post-tamoxifen.

Sox2 deletion from mature Type II hair cells altered the morphology of the afferent terminals they contacted

We were curious whether the transition of Type II hair cells toward the Type I phenotype after *Sox2* deletion induced the primary afferent neurons contacting them to shift their terminal morphology from bouton to calyx. First, we examined effects in the extrastriola (MES and LES), where the vast majority of afferent nerves are dimorphic, i.e., they have both afferent calyx and bouton nerve terminals (Fernández et al., 1990; Goldberg et al., 1990). We immunolabeled utricles for Tubb3, which is abundant in all afferent terminals. We scored Tomato-positive cells as "with a calyx" if they had Tubb3 label that surrounded all of the cell body at the level of the nucleus; in most cells, Tubb3 label extended up the cell's neck (Fig. 5*C*). In *Sox2* WT mice, very few Tomato-positive hair cells had a calyx at four months post-tamoxifen (Fig. 5*A1–A4*) and later (Fig. 5*D*), which was expected because most Tomato-positive hair cells were Type II. *Sox2* CKO induced a significant increase in the numbers of Tomato-positive hair cells with a calyx (Fig. 5*B1–B4*,*D*). Two-way ANOVA revealed significant effects of genotype ($p < 0.0002$, $f = 28.32$) and time post-tamoxifen ($p = 0.0014$, $f = 11.93$; Fig. 5*D*). Numbers of Tomato-positive hair cells with a calyx did not increase significantly in *Sox2* CKO mice relative to *Sox2* WTs until eight months post-tamoxifen, and they increased significantly in *Sox2* CKO mice between one and eight months, and between four and eight months, post-tamoxifen.

In the extrastriolar regions of *Sox2* CKO mice, we also observed Tomato-positive hair cells in which continuous Tubb3 labeling was present over only a portion (~20–70%) of the cell body at the level of the nucleus (Fig. 5*E*; illustrated in Fig. 5*F*). These structures resembled partial calyces, which are common in developing mammals but are rarely seen in adults (Favre and Sans, 1979; Rüsch et al., 1998; Warchol et al., 2019). Tubb3 antibodies also labeled boutons, and some boutons were aligned on WT hair cells so as to resemble partial calyces. Therefore, we could not reliably compare partial calyces in the extrastriola between *Sox2* WT and CKO mice in a rigorous, quantitative manner.

To explore these structures further, we examined utricular cross-sections using TEM (Fig. 5*G–O*). In these images, afferent

neural structures in contact with hair cells are highlighted in blue. In *Sox2* WT mice, sectioned Type II hair cells had discrete afferent bouton terminals contacting the basal half of their cell body (Fig. 5*G*), and in some sections, displayed no neural elements (Fig. 5*H*). Type I hair cells had a calyx terminal that surrounded the entire cell body from the base to almost the top of the neck with no breaks in calyx structure (Fig. 5*G*, *I*). By contrast, in *Sox2* CKO mice, many Type II-like hair cells (with a thick neck and apically located nucleus) were partial wrapped by continuous afferent nerve resembling a calyx (Fig. 5*J*, *K*). These cells with both Type I and Type II properties ("hybrids") had various forms of afferent terminals. In some, the partial calyx wrapped the apical portion of the hair cell body, and there were small breaks in the basal portion that were in contact with supporting cells (Fig. 5*J*,*O*) or afferent bouton terminals (Fig. 5*O*). We also noted cases in which a patch of hair cell cytoplasm seemed to be pinched between two stretches of presumably new calyx (Fig. 5*N*). In other hair cells, the calyx wrapped only the cell's base (Fig. 5*K*). We detected cells with partial calyces as early as one month (Fig. 5*N*,*O*) and as late as nine months (Fig. 5*J*,*K*) post-tamoxifen. It is important to note that hybrid cells were never seen in adult *Sox2* WT mice. However, we readily detected them using TEM in C57Bl6/J mice at postnatal day (P)14–P18 (Fig. 5*L*,*M*), and they were described in prior studies for mice at earlier postnatal stages (Rüsch et al., 1998; Warchol et al., 2019). We conclude that these hybrid cells are converting Type II hair cells (II-c), in the process of acquiring Type I-like properties in response to *Sox2* deletion.

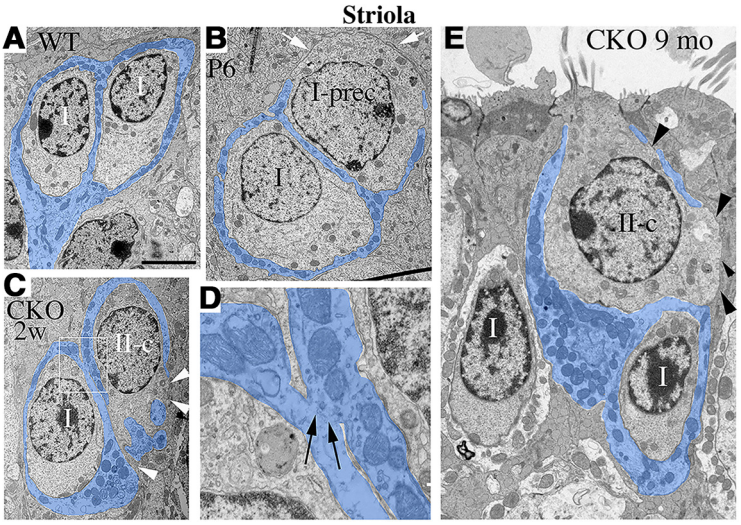

Figure 7. Type II hair cells in the striola joined calyx-only afferents following *Sox2* deletion: evidence with TEM. All panels show TEM images, with calyx afferents pseudo-colored in blue. ***A***, An exemplary complex calyx wrapping two Type I hair cells (I) from a *Sox2* WT mouse. ***B***, A developing complex calyx in a P6 mouse utricle. Arrows point to region of a Type I hair cell precursor (I-prec) that is not wrapped by calyx. ***C–E***, Two converting Type II hair cells (II-c) with a partial calyx derived from a neighboring Type I hair cell at two weeks (***C***) and nine months (***E***) after *Sox2* CKO. Arrowheads point to regions of the converting Type II hair cells not wrapped by calyx. ***D***, The boxed area in ***C*** is shown at higher magnification; arrows indicate the point where the full calyx on a Type I hair cell (left) branches to partially wrap the adjacent converting Type II hair cell (right). I, Type I hair cell. Scale bar in ***A***: 5 μm (***A***, ***C***) 4 μm (***B***), and 3 μm (***E***).

Next, we analyzed calyces on Tomato-positive hair cells in the striola. We used antibodies to Calb2 to selectively label calyx-only afferents, which receive inputs from only Type I hair cells and are confined to the striola (Fig. 6*A*,*B*; Desai et al., 2005; Li et al., 2008; Hoffman et al., 2018). Some Calb2-positive afferents wrap more than one Type I hair cell and are called complex calyx afferents (illustrated in Figs. 1*B*, 6*G*). This analysis did not quantify calyces that originated from dimorphic afferents in the striola.

In *Sox2* WT mice, very few Tomato-positive striolar hair cells had a Calb2-positive calyx (Fig. 6*C*, four months post-tamoxifen is shown, *H*), and this was consistent over time post-tamoxifen (Fig. 6*H*). This finding was anticipated for normal Type II hair cells. By contrast, many Tomato-positive striolar hair cells in *Sox2* CKO mice were fully wrapped by a Calb2-positive calyx (Fig. 6*E*, four months post-tamoxifen is shown, *H*). Two-way ANOVA revealed significant effects of genotype ($p < 0.0001$, $f = 68.31$) and time post-tamoxifen ($p = 0.0267$, $f = 4.18$). Specifically, numbers of Tomato-positive hair cells with a calyx did not increase significantly in the striola of *Sox2* CKO mice relative to *Sox2* WTs until four months post-tamoxifen, and they did not increase significantly in *Sox2* CKO mice between four and eight months post-tamoxifen. We also noted that Tomato-positive hair cells in the striola of *Sox2* CKO mice had reduced nuclear Calb2 IF, a Type II-specific property (compare Fig. 6*C*, arrow, and *E*, arrows; see also Fig. 6*C*,*E*, insets). This finding is similar to our observations in the extrastriola of *Sox2* CKO mice (Fig. 2*A1–D*).

We analyzed utricles using a second calyx marker, calbindin (Calb1), which in rodents is expressed only in calyces located in the striola and in a small region lying adjacent to the striola called the juxtastriola (Cunningham et al., 2002; Leonard and Kevetter, 2002; Prins et al., 2020). Our findings confirmed that many converting Tomato-positive Type II hair cells in the striola had gained a full calyx after *Sox2* deletion (compare Fig. 6*D* and *F*, four months post-tamoxifen is shown).

In *Sox2* CKO samples as early as one month post-tamoxifen, we found evidence with both Calb1 labeling (Fig. 6*I*, top panel) and Calb2 labeling (Fig. 6*I*, bottom panel) that afferent fibers deriving from a complex calyx (comprised of two or more continuous calyces) had partially wrapped adjacent Tomato-positive hair cells, suggesting that they were "recruiting" them to join the complex calyx afferent (Fig. 6*J*). We never detected Tomato-positive cells with these partial calyces in *Sox2* WT mice, but we saw them in *Sox2* CKO mice at all times post-tamoxifen (Fig. 6*K*).

We used TEM to further explore these changes in the striola. In *Sox2* WT mice, complex calyx afferents were readily detected (Fig. 7*A*). In all cases, the cell body of every Type I hair cell in the complex was fully wrapped by neural material; no partial calyces were seen. As a reference for how Type II hair cells might be recruited by a nearby calyx afferent to create a complex calyx after *Sox2* deletion in adulthood, we studied neonatal utricles in which striolar calyces were developing (Warchol et al., 2019). Figure 7*B* shows a calyx afferent from a striolar Type I hair cell at P6 that extends to partially wrap an adjacent Type I hair cell precursor. We found similar developing calyceal structures in *Sox2* CKO mice at two weeks post-tamoxifen (Fig. 7*C*,*D*). Neural material had branched from one calyx to partially wrap an adjacent hair cell that was Type II-like based on its afferent boutons. Similar structures were seen as late as nine months post-tamoxifen (Fig. 7*E*). These findings demonstrated that new calyces were formed on striolar Type II hair cells from branches of adjacent

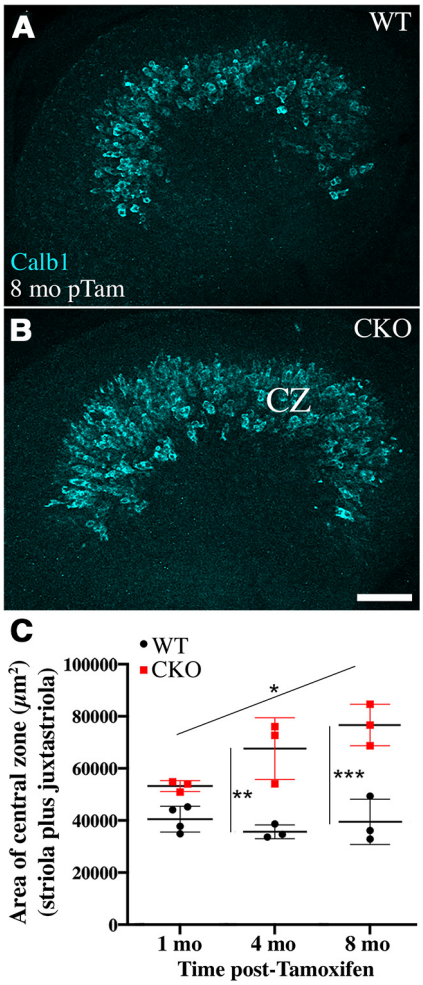

Figure 8. The aea of the central Calb1-positive region increased as Type II hair cells converted to Type I hair cells and joined, or formed, new calyces after *Sox2* deletion. ***A***, ***B***, Calbindin (Calb1) immunolabeling (cyan) reveals that the central zone (CZ) of the utricle (striola plus juxtastriola) increases in width in *Sox2* CKO relative to *Sox2* WT utricles (eight months post-tamoxifen is shown). ***C***, Graph shows the area (μm^2) of the central zone (mean ± SD) in *Sox2* WT and CKO mice at one, four, and eight months post-tamoxifen. Each point is the average number for each mouse in the group; for all groups, $n = 3$ mice except for *Sox2* WT mice at one month post-Tam, where $n = 4$; *$p < 0.05$, **$p < 0.01$, ***$p < 0.001$. Scale bar in ***B*** (lower right corner): 100 μm (***A***, ***B***).

calyces after *Sox2* CKO, and calyx formation were occurring at early and late times after tamoxifen treatment.

Based on these observations, we hypothesized that the addition of Type I hair cells to the central region of the utricle (striola plus juxtastriola) might increase its size. To investigate this, we labeled utricles with antibodies to Calb1, which as described above, marks both striolar and juxtastriolar regions (Cunningham et al., 2002; Prins et al., 2020). The area of the Calb1-positive region increased significantly in *Sox2* CKO mice relative to *Sox2* WT mice by four months post-tamoxifen and remained elevated at eight months post-tamoxifen (Fig. 8*A–C*). Two-way ANOVA revealed a significant effect of genotype ($p < 0.0001$, $f = 52.30$) but no significant effect of time post-tamoxifen ($p = 0.0732$, $f = 3.219$) This expansion was also evident in utricles that were labeled with antibodies to Calb2, a marker of calyces in the striola (Fig. 6*A*,*B*).

Type II hair cells with *Sox2* deletion adopt nuclear properties of Type I hair cells

To further explore the extent of Type II-to-Type I hair cell conversion after *Sox2* deletion, we examined the nucleus, which has a different appearance in Type I versus Type II hair cells. We measured nuclear size (area) in the same Tomato-positive extrastriolar hair cells as for the Calb2 intensity analysis in Figure 2. We noted that, in *Sox2* WT mice, the nuclear area of Type II hair cells was larger than that of Type I hair cells (Fig. 9*A1–B2*,*L*), and it did not change over time post-tamoxifen (Fig. 9*L*). By contrast, the nuclear area of Type II hair cells was smaller after *Sox2* deletion, more closely resembling Type I hair cells (compare Fig. 9*A1*,*A2* and *C1*,*C2*,*L*). As expected, the area of Type I hair cell nuclei did not differ between *Sox2* WT and CKO mice (4 months post-tamoxifen is shown) (compare Fig. 9*B1*,*B2* and *D1*,*D2*,*L*). Two-way ANOVA revealed a significant effect of genotype ($p < 0.0001$, $f = 57.65$) but not time post-tamoxifen ($p = 0.8762$, $f = 0.1334$) for the nuclear area of Type II hair cells (excluding Type I hair cell data in Fig. 9*L*). Specifically, the nuclear areas of Type II hair cells with *Sox2* CKO mice were smaller than *Sox2* WT mice at one and four months post-tamoxifen, but not at eight months post-tamoxifen. This latter finding suggests nuclear area increased over time after *Sox2* deletion to more closely resemble normal Type II hair cells. However, this interpretation is refuted by the lack of significant difference between *Sox2* CKO groups over time.

Next, we used TEM to explore the chromatin structure of converting hair cells (identified as Type II-like cells with a partial calyx) after *Sox2* deletion. Heterochromatin is transcriptionally inactive (for review, see Schueler and Sullivan, 2006; Eymery et al., 2009). It is electron-dense and therefore appears dark in TEM images. In adult *Sox2* WT mice, heterochromatin was distributed in large or small clumps throughout the nucleus of Type I hair cells (Fig. 9*E*,*G*). By contrast, in Type II hair cells, clumps of heterochromatin were usually limited to the nuclear periphery, and chromatin in the center of the nucleus was a more uniform mix of euchromatin and heterochromatin (Fig. 9*E*,*F*). These different distributions of heterochromatin in vestibular Type I and Type II hair cells were previously reported in neonatal mice (Rüsch et al., 1998). As early as two weeks after tamoxifen in *Sox2* CKO mice, converting Type II hair cells (i.e., those with a partial calyx) had clumps of heterochromatin that more closely resembled Type I hair cells (Fig. 9*H*). Similar cells were seen at nine months after tamoxifen in *Sox2* CKO mice (Fig. 9*I–K*). These observations indicated that *Sox2* deletion from Type II hair cells caused them to acquire nuclear features typical of Type I hair cells.

Sox2 deletion from Type II hair cells induced the stereocilia and synapses to resemble Type I hair cells

To further explore the extent of conversion to a Type I-like phenotype, we examined the stereocilia, the sensory organelles of hair cells, following *Sox2* deletion. Prior studies showed that the stereocilia of Type I hair cells in mice are considerably thicker than those of Type II hair cells (Rüsch et al., 1998; Li et al., 2008), and we found this to be true in *Sox2* WT controls using TEM (unpaired Student's *t* test, $p < 0.0001$, $t = 7.002$, df = 14; Fig. 10*A*, *B*,*C*,*E*,*F*). By contrast, the stereocilia of converting Type II hair cells (with a partial calyx) in *Sox2* CKO mice at one month post-tamoxifen were considerably thicker than *Sox2* WT Type II hair cells and more closely resembled Type I hair cell stereocilia (Fig. 10*A*,*D*,*G*,*H*). Two-way ANOVA of *Sox2* CKO mice showed significant differences across cell types (Type I, Type II, and converting Type II; $p < 0.0001$, $f = 30.45$) and time post-tamoxifen ($p = 0.0037$, $f = 9.61$). In both the one month and the five to nine months post-tamoxifen groups, the stereocilia of Type I hair cells were significantly thicker than those of Type II hair cells,

but they were not significantly thicker than converting Type II hair cells. In both groups, the stereocilia of converting hair cells were significantly thicker than Type II hair cells. There was no significant change in the thickness of stereocilia in converting hair cell types between one and five to nine months.

We also used TEM to explore whether synaptic ribbons shifted from Type II-like to Type I-like following *Sox2* deletion. Ribbons are the presynaptic element in the vestibular hair cell-afferent nerve synapse (for review, see Moser et al., 2006). Ribbon morphology in each hair cell type is similar in some respects: both are composed of an electron-dense central region surrounded by synaptic vesicles. Our analysis of hundreds of hair cells from all zones of adult *Sox2* WT mouse utricles demonstrated that ribbon synapses in Type I hair cells were either (1) single bar-shaped ribbons located close to the plasma membrane (Fig. 10*I*, top box, *J*) or (2) multiple ribbons that were clustered together and not apposed to a differentiated postsynaptic membrane (Fig. 10*L*). By contrast, ribbons in adult Type II hair cells in *Sox2* WT mice were round or ovoid (Fig. 10*I*, bottom, box, *K*; Pujol et al., 2014). We never detected bar-type or clustered ribbons in *Sox2* WT Type II hair cells in adult mice. However, investigators have described these forms of ribbons in Type II hair cells in chinchilla (Lysakowski and Goldberg, 1997).

Following *Sox2* deletion from Type II hair cells, we used TEM to examine synapses in hair cells with partial calyces, which we assumed to be converting into Type I hair cells. In these cells, synaptic ribbons were either ovoid, as in normal Type II hair cells (data not shown), or bar-shaped, as in normal Type I hair cells (Fig. 10*M*,*N*). Furthermore, ribbons in converting hair cells were located near afferent nerve terminals that appeared larger than the typical bouton afferent, resembling a growing calyx afferent (Fig. 10*M*,*N*). We also detected some converting cells with highly enlarged round or ovoid ribbons that were located in the cell's most basal portion and sometimes relatively far from the plasma membrane, or "floating" (Fig. 10*O*,*P*). These ribbons may have been undergoing remodeling as the Type II hair cell basolateral process retracted and the calyx grew around the converting hair cell. Altogether, our observations of synapses support the interpretation that *Sox2* deletion from Type II hair cells causes them to adopt Type I-like synaptic ribbons.

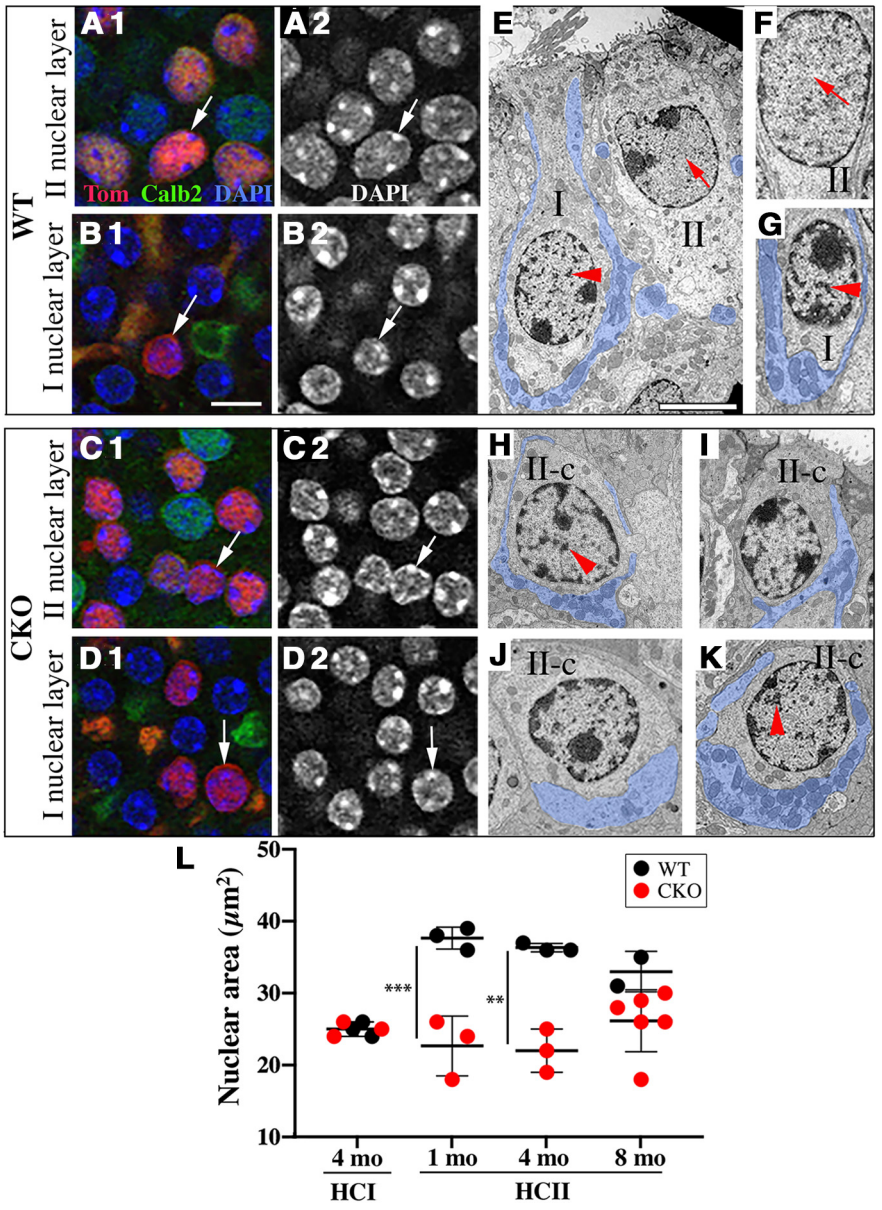

Figure 9. Converting hair cells acquired additional Type I-like features: changes in nuclear size and heterochromatin distribution. ***A1–D2***, Confocal images of the Type I and Type II hair cell nuclear layers (Fig. 1*B* for reference) in the extrastriola of *Sox2* WT and CKO mice at four months post-tamoxifen. ***A1***, ***B1***, ***C1***, ***D1***, Tomato (magenta), Calb2 (green), and DAPI (blue) labeling. ***A2***, ***B2***, ***C2***, ***D2***, DAPI labeling (white) only for each corresponding field. Arrows point to the same nuclei for each set of images (e.g., ***A1***, ***A2***). ***E***, ***F***, TEM images of exemplary Type I and Type II hair cells from *Sox2* WT utricles. Red arrowheads in ***E***, ***G*** point to small clumps of heterochromatin in each Type I nucleus, and red arrows in ***E***, ***F*** point to areas in Type II nuclei lacking heterochromatin clumps**.** ***H–K***, TEM images of four exemplary converting Type II HCs (II-c) at two weeks post-tamoxifen (***H***) and at nine months post-tamoxifen (***I–K***). Each hair cell has a partial calyx (pseudo-colored in blue). Red arrowheads in ***H***, ***K*** point to examples of small clumps of heterochromatin in each cell's nucleus. HCI, Type I hair cells; HCII, Type II hair cells; mo, months. Scale bar in ***B1***: 5 μm (*A1–D2*); in ***E***: 5 μm (***E–K***). ***L***, Graph shows nuclear area (mean ± SD) for Tomato-labeled Type I and Type II hair cells for *Sox2* WT and CKO mice at various times post-tamoxifen. Each point is the average number for each mouse in the group; for all groups, $n = 3$ mice except for *Sox2* WT at eight months post-Tamoxifen, $n = 2$ and for *Sox2* CKO at eight months post-Tam, $n = 6$; $^{**}p < 0.01$, $^{***}p < 0.001$.

Spatiotemporal progression of Type II-to-Type I conversion after *Sox2* deletion

In an effort to better understand the steps by which Type II hair cells converted into Type I-like hair cells after *Sox2* deletion, we performed three additional analyses. First, we compared two

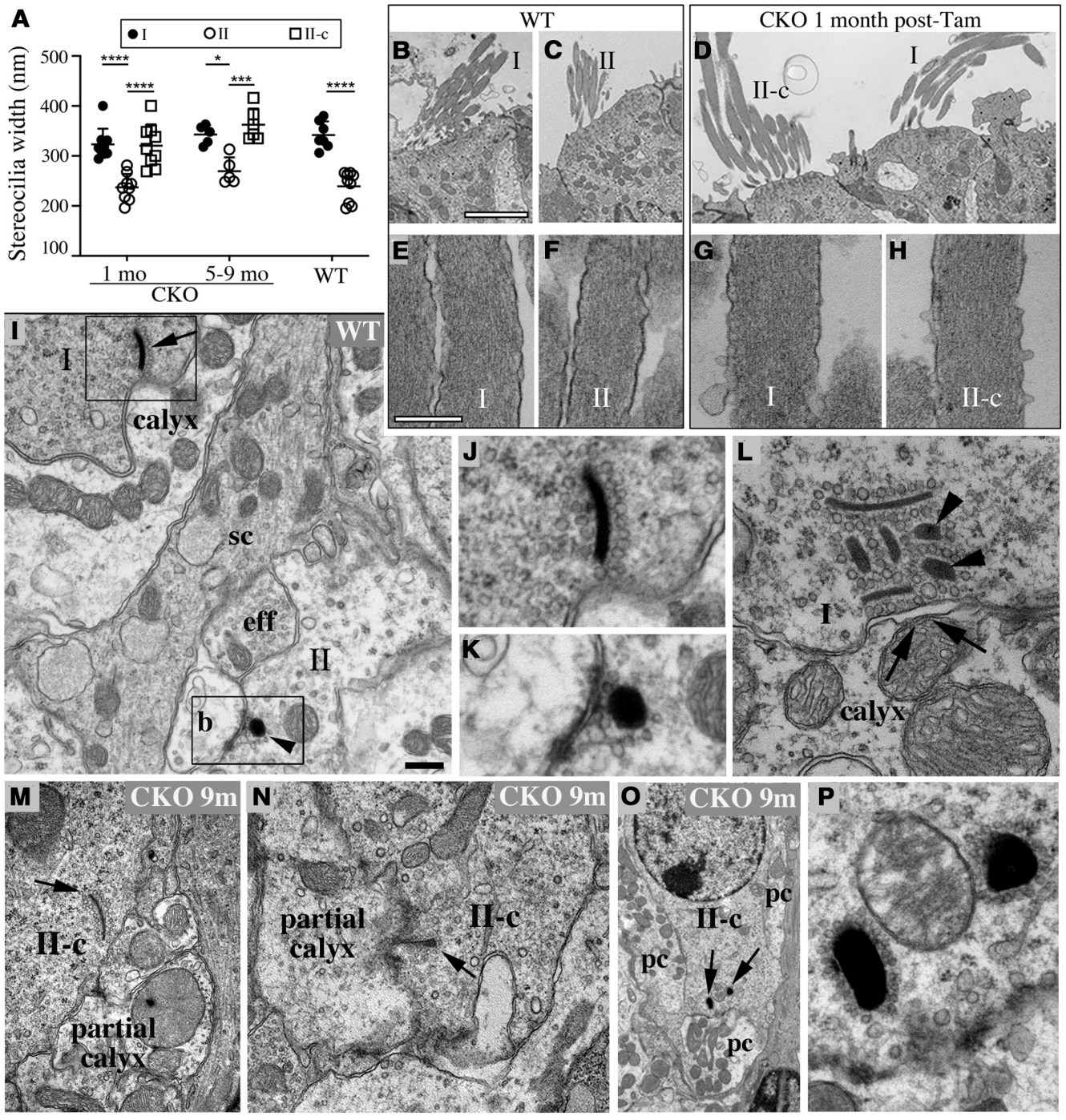

Figure 10. Stereocilia width and synaptic ribbons in Type II hair cells become more Type I-like after *Sox2* deletion. ***A***, Graph shows stereocilia width (nm; mean ± SD) for Type I and Type II hair cells from *Sox2* WT mice, and for Type I, Type II, and Type II-converting (II-c) hair cells from *Sox2* CKO mice at one month or five to nine months post-tamoxifen. For this analysis, we examined: seven Type I hair cells and nine Type II hair cells from five *Sox2* WT mice; nine Type I hair cells, nine Type II hair cells, and nine converting Type II hair cells from three *Sox2* CKO mice at one month; and five Type I hair cells, five Type II hair cells, and six converting Type II hair cells from six *Sox2* CKO mice at five to nine months; $^{*}p < 0.05$, $^{***}p < 0.001$, $^{****}p < 0.0001$. ***B***, ***C***, TEM images show the typical appearance of stereocilia in *Sox2* WT mice, with Type I hair cell stereocilia (***B***) considerably thicker than Type II hair cell stereocilia (***C***). Images were taken from the extrastriola. ***D***, Stereocilia on a converting Type II hair cell (II-c, left, identified by its partial calyx; not shown) after *Sox2* CKO appear to be as thick or thicker than those on the adjacent Type I hair cell on the right (identified by its full calyx; not shown). ***E–H***, Higher-magnification TEM images of stereocilia from *Sox2* WT (***E***, ***F***) and CKO (***G***, ***H***) hair cells. ***I***, TEM images of two hair cells from a *Sox2* WT mouse, a Type I hair cell (***I***) in the upper left and a Type II hair cell (II) in the lower right. The black arrow points to a bar-type ribbon in the Type I hair cell with the afferent calyx located below the hair cell plasma membrane. The black arrowhead points to a round ribbon in a Type II hair cell with a bouton (b) located to the left of the hair cell plasma membrane. A vestibular efferent (eff) sits slightly above the bouton. ***J***, ***K***, Higher magnifications of the boxed areas in I showing a bar-type ribbon in the Type I hair cell (***J***) and a round synapse in the Type II hair cell (***K***). ***L***, Cluster-type ribbon in a Type I hair cell. Arrowheads point to the central core of the ribbon, and arrows point to the calyx plasma membrane, which in this section lacks a postsynaptic specialization. ***M–P***, TEM images of converting hair cells (II-c) from *Sox2* CKO mice at nine months post-tamoxifen. Arrows in ***M***, ***N*** point to bar-like ribbons located close to partial calyx in two different converting cells. ***O***, Low-magnification TEM image showing a converting Type II hair cell contacted by three partial calyces (pc). Arrows point to two enlarged ovoid floating ribbons. ***P***, Enlargement of region in O that is indicated by arrows. Type I, Type I hair cell; II, Type II hair cell; c, calyx afferent; b, bouton afferent; eff, efferent presynapse; sc, supporting cell. Scale bars in ***B***: 3 μm (***B–D***); in ***E***: 250 nm (***E–H***); and in ***I***: 200 nm (***I***, ***M***, ***N***), 100 nm (***J–L***, ***P***), and 400 nm (***O***).

phenotypic features, Calb2 IF intensity (Fig. 2) and nuclear area (Fig. 9), in *Sox2* WT and CKO mice at different times following tamoxifen. We measured each feature in the same Tomato-labeled nucleus in either the Type I layer or the Type II layer (Fig. 11*A*). In *Sox2* WT mice, as expected, Type I hair cells at each time post-tamoxifen (gray-scale circles) had significantly smaller nuclei and lower Calb2 intensity than Type II hair cell nuclei (orange-red-scale circles). By contrast, Type II hair cells in *Sox2* CKO mice (blue-green scale circles) had reduced Calb2 intensity and smaller nuclei. A Pearson correlation test showed that the two variables were significantly associated ($r = 0.6929$, $p = 0.0007$). Interestingly, though, not all mice with *Sox2* deletion changed to the same degree over time post-tamoxifen. For example, some *Sox2* CKO mice had, on average, larger nuclei at eight months post-Tamoxifen than did *Sox2* CKO mice at four months post-tamoxifen (also see Fig. 9).

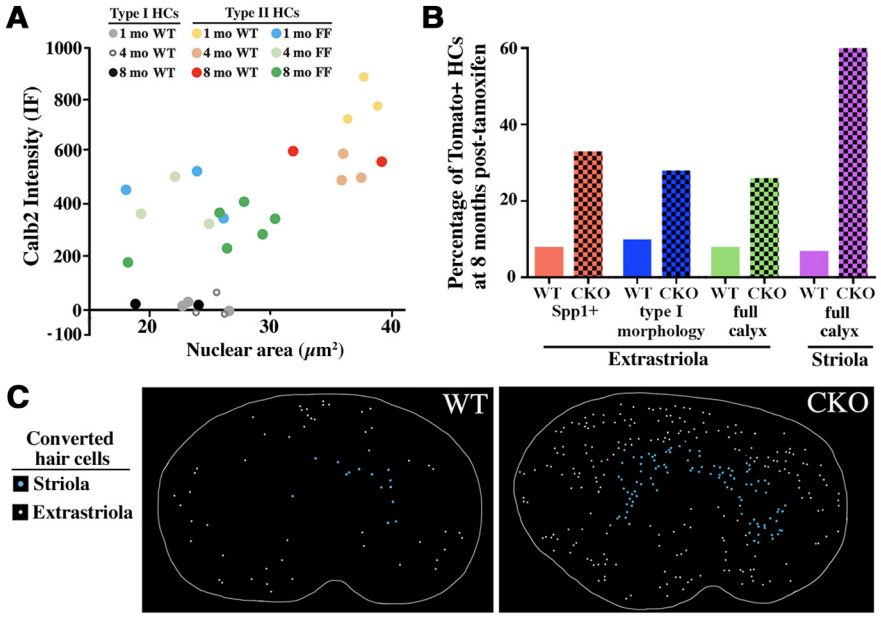

Figure 11. Spatiotemporal patterns of Type I-to-Type II conversion after *Sox2* deletion. ***A***, Graph shows mean values per animal for nuclear area and Calb2 IF intensity for Tomato-labeled Type I and Type II hair cells from *Sox2* WT and Tomato-labeled Type II-layer hair cells *Sox2* CKO mice at various times post-tamoxifen. ***B***, Graph shows percentage of (1) Tomato-positive cells in the extrastriola that were Spp1-positive (red bars), had a Type I morphology (blue bars), or had a calyx (green bars); and (2) Tomato-positive cells in the striola with a calyx (magenta bars). All data are from *Sox2* WT or CKO mice at eight months post-tamoxifen. ***C***, Maps of Tomato-positive Type I-like hair cells from a representative *Sox2* WT and CKO utricle at four months post-tamoxifen. Striolar hair cells (located in the Calb2 zone) are represented by blue dots, while extrastriolar hair cells are shown as white dots.

Next, we examined the percentage of Tomato-labeled Type II hair cells with *Sox2* deletion that acquired various Type I-specific features by eight months post-tamoxifen (Fig. 11*B*; Table 3). Because a small proportion of Type I hair cells in *Sox2* WT controls expressed Cre, 8–10% of Tomato-positive extrastriolar hair cells were Spp1-positive, had Type I-like morphology, and/or were contacted by a calyx-type afferent as defined by Tubb3 labeling. After *Sox2* deletion, a higher percentage of Tomato-positive extrastriolar hair cells had Type I-like features: 33% were Spp1-positive, 28% had a Type I-like morphology, and 26% had a calyx. The variation in these percentages suggested that each feature changed to a different extent within each hair cell. Interestingly, a higher percentage of Tomato-positive hair cells in the striola (60%) acquired a full calyx than in the extrastriola (26%).

Finally, we assessed spatial patterns of Type II-to-Type I conversion in *Sox2* CKO mice by generating maps of Tomato-positive Type I-like hair cells from one representative utricle from *Sox2* WT and CKO mice at four months post-tamoxifen (Fig. 11*C*), defining Tomato-positive hair cells as Type I-like if (1) in the extrastriola, they had Type I morphology (described in association with Fig. 4) and (2) in the striola, they had a Calb2-positive calyx (described in association with Fig. 6). Tomato-positive Type I-like hair cells were distributed throughout the utricle, with higher numbers in *Sox2* CKO mice relative to *Sox2* WT mice. We estimated that, at eight to nine months post-tamoxifen, the conversion of Type II hair cells to Type I hair cells increased the total number of Type I hair cells by 13% in the extrastriola (Table 4) and 21% in the striola (Table 5), and decreased the total number of Type II hair cells by the same amounts.

Table 3. Estimated percentages of tomato+ HCs with each feature (Fig. 11B)

		Time post-Tam	*Sox2* WT	*Sox2* CKO
Extrastriola	Number of Tom+ HCs per utricle	8 months	786	882
Striola	Number of Tom+ HCs per utricle	8 months	202	151
	% of Tom+ HCs with Spp1 label	8 months	8%	33%
Extrastriola	% of Tom+ HCs with HCI shape	8 months	10%	28%
	% of Tom+ HCs with calyx	8 months	8%	26%
Striola	% of Tom+ HCs with calyx	8 months	7%	60%

Percentages were calculated using top two rows as denominator and data from corresponding graphs as numerator.

Discussion

There are four types of hair cells in mammals: inner and outer hair cells in the cochlea, and Type I and Type II hair cells in the vestibular organs. Investigators recently identified three transcription factors (*Ikzf2*, *Insm1*, and *Sox2*) that control the differentiation of cochlear or vestibular hair cells into specific types during inner ear development (Chessum et al., 2018; Wiwatpanit et al., 2018; Lu et al., 2019). Here, we demonstrate that *Sox2* is required to maintain the specific properties of Type II vestibular hair cells in adulthood. Conditional deletion of *Sox2* from mature Type II hair cells mice revealed unexpected plasticity, causing them to lose a constellation of Type II-specific features and to acquire several properties unique to Type I hair cells. To our knowledge, this is the first evidence of a gene that is required in mature hair cells to maintain their type-specific, differentiated state.

We also found that *Sox2* deletion from Type II hair cells induced dramatic changes in vestibular afferent terminals that are postsynaptic to hair cells, shifting their morphology from bouton to calyx. Remarkably, neurons that underwent this switch experienced no genetic change; rather, they responded to a phenotypic switch or drift in their presynaptic partners, the hair cells. Prior studies showed that healthy inputs from the mature inner ear are required to maintain the structure and biochemical

Table 4. Estimates of percent increase in extrastriolar HCI per utricle

Time post-Tam	Extrastriolar Tom+ HCI from Figure 4, *Sox2* WT	Extrastriolar Tom+ HCI from Figure 4, *Sox2* CKO	Increase in Tom+ ES HCI *Sox2* CKO re. WT**	Estimated % increase in ES HCI number*
1 month	64	152	88	7%
4 months	54	201	147	11%
8 months	80	250	170	13%

* Estimates of % increase were calculated as follows: we counted, on average, 1113 ES HCII (Tom− or Tom+) per WT utricle ($n = 3$ mice at 4 months post-Tam). Based on the ratio of HCI to HCII in ES (1.19–1.00 from Desai et al., 2005), we estimated there are 1324 ES HCI per WT utricle. We added 1324 to the number by which ES HCI increased after Sox2 CKO** and divided by 1324 to determine the % increase.
** Difference between the second and third columns.

Table 5. Estimates of percent increase in striolar HCI per utricle

Time post-Tam	Striolar Tom+ HCI from Figure 6, *Sox2* WT	Striolar Tom+ HCI from Figure 6, *Sox2* CKO	Increase in Tom+ striolar HCI *Sox2* CKO re. WT**	Estimated % Increase in striolar HCI number*
1 month	13	46	33	9%
4 months	15	71	56	16%
8 months	15	91	76	21%

* Estimates of % increase were calculated as follows: we counted, on average, 245 striolar HCII (Tom− or Tom+) per utricle ($n = 3$ mice at 4 months post-Tam). Based on the ratio of HCI to HCII in striola (1.47–1.00 from Desai et al., 2005), we estimated there are 360 striolar HCI per utricle. We added 360 to the number by which ES HCI increased after Sox2 CKO** and divided by 360 to determine the % increase.
** Difference between the second and third columns.

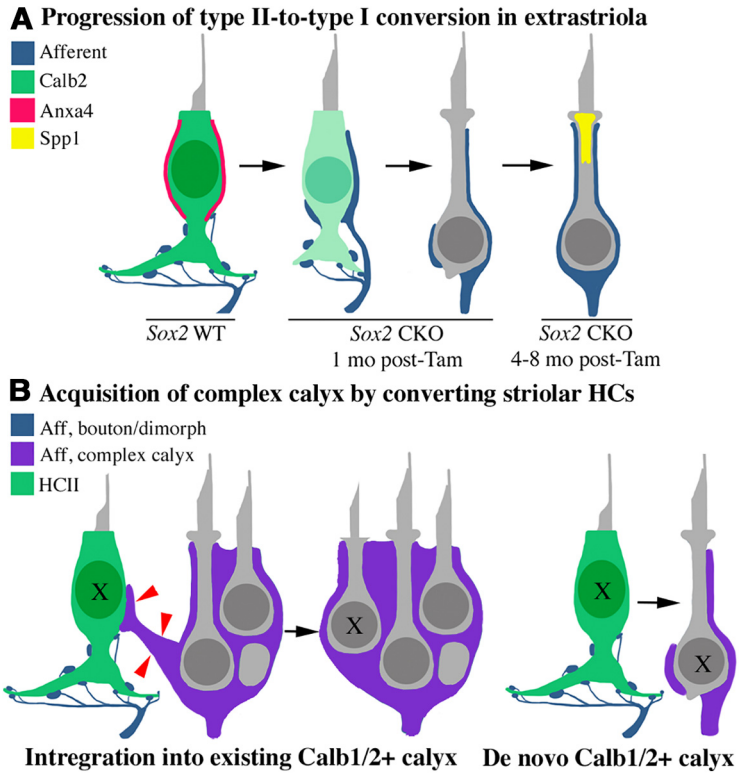

Figure 12. Theoretical models for Type II-to-Type I hair cell conversion and for calyx acquisition following *Sox2* deletion. ***A***, This model demonstrates how Type II hair cells in the extrastriola may progress toward a Type I-like fate over time after *Sox2* deletion. At one month post-tamoxifen, some converting hair cells have a mix of boutons and partial calyx afferent innervation. They have reduced Calb2 and Anxa4 and thicker stereocilia, but they still resemble Type II hair cells (e.g., they have an apically located nucleus and basolateral processes). Other hair cells observed at this same time resemble Type I hair cells morphologically (thin neck, more basal nuclear position) and have lost the synaptic boutons, basolateral processes, and Calb2 expression. By four to eight months post-tamoxifen, converting hair cells have gained Spp1 expression, have a calyx, and more closely resemble Type I hair cells, morphologically. ***B***, This model shows how vestibular afferent nerves in the striola may approach a converting Type II hair cell following *Sox2* deletion. On the left, a neurite (red arrows) extends from a complex calyx to approach a Type II hair cell (marked by X in its nucleus) after *Sox2* deletion, and that hair cell is incorporated into the complex calyx as it converts. On the right, a Type II hair cell acquires a new calyx that is positive for a calyx-only fiber marker (Calb1 or Calb2), perhaps dictated by its regional identity.

properties of neurons in ascending pathways of the cochlear and vestibular sensory systems. For example, dramatic dendritic remodeling in auditory brainstem neurons occurs in chickens after deafferentation caused by cochlear ablation, tetrodotoxin-mediated primary afferent silencing, or central tract cutting (Wang and Rubel, 2012). Our findings show that deletion of a single transcription factor from adult vestibular hair cells is sufficient to induce afferent terminal remodeling, which emphasizes the powerful role that hair cells, specifically, play in regulating afferent neuron morphology in the inner ear.

Sox2 is required to maintain the Type II hair cells in adult mice

In utricles of adult mice, there is a low level of turnover of Type II hair cells (Bucks et al., 2017). Otherwise, the hair cell population appears to be stable, and there is no evidence that hair cells transition between types, II-to-I or vice versa (Bucks et al., 2017). Following *Sox2* deletion, however, Type II hair cells in all regions of the utricle converted to Type I-like cells (schematized for the extrastriola in Fig. 12*A*). Some cellular changes occurred quickly. For instance, at one month after *Sox2* deletion, many extrastriolar Type II hair cells had lost immunoreactivity for Calb2 and Anxa4 and had acquired Type I morphology including a flask-shaped cell body, thicker stereocilia, a smaller nucleus, and increased heterochromatin density. By contrast, it took more time (four to eight months) for significant numbers of transitioning hair cells in the extrastriola to upregulate Spp1 and/or to acquire a calyx terminal, both hallmarks of Type I hair cells. Some features such as Type I morphology were detected in increasing numbers of Tomato-positive hair cells in *Sox2* CKO mice between one and eight months post-tamoxifen, while other features such as reduced Calb2 expression, first evident at one month post-tamoxifen, did not change over time.

Some Tomato-positive hair cells failed to alter key cell-specific features after *Sox2* deletion despite the loss of Sox2 protein from 98% of Tomato-labeled hair cells. For instance, 70–80% of Tomato-labeled extrastriolar hair cells did not acquire a calyx afferent or a Type I shape by eight months after *Sox2* deletion. The finding that hair cells take long and variable times to transdifferentiate after *Sox2* deletion is consistent with cell reprogramming studies in other tissues (Hanna et al., 2009). Nonetheless, we did not expect Type II hair cells in a mature, homeostatic state to show such variable responses. One possible explanation is hair cell age. In mice, Type II hair cells are born before birth (Sans and Chat, 1984), during the early postnatal period (McInturff et al., 2018; Wang et al., 2019; Warchol et al., 2019), and in adulthood (Bucks et al., 2017). Hair cells may lose responsiveness to *Sox2* deletion as they mature and age. Alternatively, there may be unrecognized subtypes of Type II hair cells that are poised at different transcriptional or epigenetic state or additional factors that compensate for the loss of *Sox2* in some cells. Single cell transcriptome analyses would clarify which Type I properties are acquired by Type II hair cells after *Sox2* deletion.

The mechanisms by which Sox2 maintains the Type II hair cell fate in adult mice are unknown. Sox2 is expressed in otic sensory progenitors (Hume et al., 2007) and is required for development of both hair cells and supporting cells (Kiernan et al., 2005; Kempfle et al., 2016). Deletion of *Sox2* from developing hair cells in vestibular organs causes them to acquire the Type I phenotype (Lu et al., 2019). Sox2 functions as both a direct regulator of gene transcription (for review, see Wegner, 1999) and a chromatin remodeler (Amador-Arjona et al., 2015). In neural progenitors, Sox2 binds to DNA regions that become transcriptionally active as neurons differentiate (Bergsland et al., 2011; Lodato et al., 2013). Sox2 may also be required to maintain the fate of some neurons after maturation (Ferri et al., 2004). While many studies have demonstrated Sox2's role as an activator of transcription, it can also repress gene transcription (Lu et al., 2014). Therefore, in vestibular Type II hair cells of adult mice, Sox2 likely maintains the Type II fate by activiating and repressing specific expression of genes at both genetic and epigenetic levels. Studies are underway to understand these mechanisms.

The morphology of vestibular afferent neurons depends on *Sox2* in presynaptic Type II hair cells

Sox2 deletion from adult Type II hair cells altered the shape of vestibular afferent nerve terminals, switching their morphology (Fig. 12*A*) and synapses from bouton type to calyx type. As this occurred, the number of Tomato-positive hair cells with a calyx increased across the utricle, with the striola preceding the extrastriola. Because we could not image the same cells over time, we do not know the steps by which neurons changed their terminals' morphology. However, TEM and confocal image analysis of the striola revealed neurite branches extending from a calyx to enwrap nearby converting Type II hair cells, which would either expand an existing complex calyx (Fig. 12*B*, left side) or generate a new complex calyx. The size of the striola and juxtastriola increased following *Sox2* CKO, as defined by Calb1 labeling. This expansion likely resulted from the mechanism shown in Figure 12*B*, left side, or from activation of Calb1 expression in single calyces as they formed *de novo* around converting hair cells in the striola or juxtastriola (Fig. 12*B*, right side), perhaps in response to zone-specific signals. Finally, new calyces may have formed from the expansion and/or merging of afferent boutons around converting hair cells.

The finding that *Sox2* deletion from adult Type II hair cells induces the loss of boutons and the acquisition of a calyx reveals that vestibular hair cells provide signals necessary to maintain the correct morphology of their postsynaptic neuronal partners. Little is known about the signals that regulate the development of vestibular afferent terminals or their maintenance in adult animals. Likely candidates are secreted proteins such as bone morphogenetic proteins (BMPs) and membrane-bound signaling molecules like Notch ligands. In mice, BMP signaling is required for development of the calyx of Held, which is a large axon terminal that has similar structure to the vestibular afferent calyx on Type I hair cells but lies presynaptic to neurons in the medial nucleus of the trapezoid body (Xiao et al., 2013; Kronander et al., 2019). Notch signaling regulates the density and morphology of dendritic spines, which are postsynaptic structures, in the brains of adult mice (Alberi et al., 2011; Prox et al., 2013). Our future studies aim to identify regulators of vestibular afferent terminal morphology by examining the transcriptomes of Type II hair cells with or without *Sox2* deletion.

Because the majority of afferent neurons are dimorphic (i.e., they receive inputs from both Type I and Type II hair cells), investigators have found it challenging to test the function of each hair cell subtype (for review, see Eatock and Songer, 2011). The findings presented here offer new opportunities to explore the specialized functions of Type I and Type II hair cells in adult mammals. By increasing the proportion of Type I-to-Type II hair cells using *Sox2* CKO mice, electrophysiological and behavioral studies could be employed to better understand the contributions of each hair cell type to afferent nerve firing properties and vestibular function. Such studies would provide fundamental knowledge that is currently lacking in the field of vestibular neurobiology.

References

Alberi L, Liu S, Wang Y, Badie R, Smith-Hicks C, Wu J, Pierfelice TJ, Abazyan B, Mattson MP, Kuhl D, Pletnikov M, Worley PF, Gaiano N (2011) Activity-induced notch signaling in neurons requires Arc/Arg3.1 and is essential for synaptic plasticity in hippocampal networks. Neuron 69:437–444.

Amador-Arjona A, Cimadamore F, Huang CT, Wright R, Lewis S, Gage FH, Terskikh AV (2015) SOX2 primes the epigenetic landscape in neural precursors enabling proper gene activation during hippocampal neurogenesis. Proc Natl Acad Sci USA 112:E1936–E1945.

Bergsland M, Ramsköld D, Zaouter C, Klum S, Sandberg R, Muhr J (2011) Sequentially acting Sox transcription factors in neural lineage development. Genes Dev 25:2453–2464.

Bucks SA, Cox BC, Vlosich BA, Manning JP, Nguyen TB, Stone JS (2017) Supporting cells remove and replace sensory receptor hair cells in a balance organ of adult mice. Elife 6:e18128.

Burns JC, On D, Baker W, Collado MS, Corwin JT (2012) Over half the hair cells in the mouse utricle first appear after birth, with significant numbers originating from early postnatal mitotic production in peripheral and striolar growth zones. J Assoc Res Otolaryngol 13:609–627.

Burns JC, Stone JS (2017) Development and regeneration of vestibular hair cells in mammals. Semin Cell Dev Biol 65:96–105.

Chessum L, Matern MS, Kelly MC, Johnson SL, Ogawa Y, Milon B, McMurray M, Driver EC, Parker A, Song Y, Codner G, Esapa CT, Prescott J, Trent G, Wells S, Dragich AK, Frolenkov GI, Kelley MW, Marcotti W, Brown SDM, et al. (2018) Helios is a key transcriptional regulator of outer hair cell maturation. Nature 563:696–700.

Chow LML, Tian Y, Weber T, Corbett M, Zuo J, Baker SJ (2006) Inducible Cre recombinase activity in mouse cerebellar granule cell precursors and inner ear hair cells. Dev Dyn 235:2991–2998.

Cunningham LL, Cheng AG, Rubel EW (2002) Caspase activation in hair cells of the mouse utricle exposed to neomycin. J Neurosci 22:8532–8540.

Desai SS, Zeh C, Lysakowski A (2005) Comparative morphology of rodent vestibular periphery. I. Saccular and utricular maculae. J Neurophysiol 93:251–266.

Eatock RA, Songer JE (2011) Vestibular hair cells and afferents: two channels for head motion signals. Annu Rev Neurosci 34:501–534.

Eymery A, Callanan M, Vourc'h C (2009) The secret message of heterochromatin: new insights into the mechanisms and function of centromeric and pericentric repeat sequence transcription. Int J Dev Biol 53:259–268.

Favre D, Sans A (1979) Morphological changes in afferent vestibular hair cell synapses during the postnatal development of the cat. J Neurocytol 8:765–775.

Faulstich BM, Onori KA, du Lac S (2004) Comparison of plasticity and development of mouse optokinetic and vestibulo-ocular reflexes suggests differential gain control mechanisms. Vision Res 44:3419–3427.

Fernández C, Goldberg JM, Baird RA (1990) The vestibular nerve of the chinchilla. III. Peripheral innervation patterns in the utricular macula. J Neurophysiol 63:767–780.

Ferri ALM, Cavallaro M, Braida D, Di Cristofano A, Canta A, Vezzani A, Ottolenghi S, Pandolfi PP, Sala M, DeBiasi S, Nicolis SK (2004) Sox2 deficiency causes neurodegeneration and impaired neurogenesis in the adult mouse brain. Development 131:3805–3819.

Goldberg JM, Desmadryl G, Baird RA, Fernández C (1990) The vestibular nerve of the chinchilla. IV. Discharge properties of utricular afferents. J Neurophysiol 63:781–790.

Hanna J, Saha K, Pando B, van Zon J, Lengner CJ, Creyghton MP, van Oudenaarden A, Jaenisch R (2009) Direct cell reprogramming is a stochastic process amenable to acceleration. Nature 462:595–601.

Hoffman LF, Choy KR, Sultemeier DR, Simmons DD (2018) Oncomodulin expression reveals new insights into the cellular organization of the murine utricle striola. J Assoc Res Otolaryngol 19:33–51.

Hume CR, Bratt DL, Oesterle EC (2007) Expression of LHX3 and SOX2 during mouse inner ear development. Gene Expr Patterns 7:798–807.

Kempfle JS, Turban JL, Edge ASB (2016) Sox2 in the differentiation of cochlear progenitor cells. Sci Rep 6:23293.

Kiernan AE, Pelling AL, Leung KKH, Tang ASP, Bell DM, Tease C, Lovell-Badge R, Steel KP, Cheah KSE (2005) Sox2 is required for sensory organ development in the mammalian inner ear. Nature 434:1031–1035.

Kirkegaard M, Nyengaard JR (2005) Stereological study of postnatal development in the mouse utricular macula. J Comp Neurol 492:132–144.

Kronander E, Clark C, Schneggenburger R (2019) Role of BMP Signaling for the formation of auditory brainstem nuclei and large auditory relay synapses. Dev Neurobiol 79:155–174.

Lapeyre P, Guilhaume A, Cazals Y (1992) Differences in hair bundles associated with type I and type II vestibular hair cells of the guinea pig saccule. Acta Otolaryngol 112:635–642.

Leonard RB, Kevetter GA (2002) Molecular probes of the vestibular nerve I. Peripheral termination patterns of calretinin, calbindin and peripherin containing fibers. Brain Res 928:8–17.

Li A, Xue J, Peterson EH (2008) Architecture of the mouse utricle: macular organization and hair bundle heights. J Neurophysiol 99:718–733.

Lodato MA, Ng CW, Wamstad JA, Cheng AW, Thai KK, Fraenkel E, Jaenisch R, Boyer LA (2013) SOX2 co-occupies distal enhancer elements with distinct POU factors in ESCs and NPCs to specify cell state. PLoS Genet 9:e1003288.

Lu J, Hu L, Ye B, Hu H, Tao Y, Shu Y, Chiang H, Borse V, Xiang M, Wu H, Edge ASB, Shi F (2019) Increased type I and decreased type II hair cells after deletion of Sox2 in the developing mouse utricle. Neuroscience 422:146–160.

Lysakowski A, Goldberg J (1997) A regional ultrastructural analysis of the cellular and synaptic architecture in the chinchilla cristae ampullares. J Comp Neurol 389:419–443.

Madisen L, Zwingman TA, Sunkin SM, Oh SW, Zariwala HA, Gu H, Ng LL, Palmiter RD, Hawrylycz MJ, Jones AR, Lein ES, Zeng H (2010) A robust and high-throughput Cre reporting and characterization system for the whole mouse brain. Nat Neurosci 13:133–140.

McInturff S, Burns JC, Kelley MW (2018) Characterization of spatial and temporal development of type I and type II hair cells in the mouse utricle using new cell-type-specific markers. Biol Open 7:bio038083.

Moser T, Brandt A, Lysakowski A (2006) Hair cell ribbon synapses. Cell Tissue Res 326:347–359.

Oesterle EC, Campbell S, Taylor RR, Forge A, Hume CR (2008) Sox2 and Jagged1 expression in normal and drug-damaged adult mouse inner ear. J Assoc Res Otolaryngol 9:65–89.

Prins TJ, Myers ZA, Saldate JJ, Hoffman LF (2020) Calbindin expression in adult vestibular epithelia. J Comp Physiol A Neuroethol Sens Neural Behav Physiol 206:623–637.

Prox J, Bernreuther C, Altmeppen H, Grendel J, Glatzel M, D'Hooge R, Stroobants S, Ahmed T, Balschun D, Willem M, Lammich S, Isbrandt D, Schweizer M, Horré K, De Strooper B, Saftig P (2013) Postnatal disruption of the disintegrin/metalloproteinase ADAM10 in brain causes epileptic seizures, learning deficits, altered spine morphology, and defective synaptic functions. J Neurosci 33:12915–12928, 12928a.

Pujol R, Pickett SB, Nguyen TB, Stone JS (2014) Large basolateral processes on type II hair cells are novel processing units in mammalian vestibular organs. J Comp Neurol 522:3141–3159.

Ruben RJ (1967) Development of the inner ear of the mouse: a radioautographic study of terminal mitoses. Acta Otolaryngol Suppl 220:1–44.

Rüsch A, Lysakowski A, Eatock RA (1998) Postnatal development of type I and type II hair cells in the mouse utricle: acquisition of voltage-gated conductances and differentiated morphology. J Neurosci 18:7487–7501.

Sans A, Chat M (1982) Analysis of temporal and spatial patterns of rat vestibular hair cell differentiation by tritiated thymidine radioautography. J Comp Neurol 206:1–8.

Schindelin J, Arganda-Carreras I, Frise E, Kaynig V, Longair M, Pietzsch T, Preibisch S, Rueden C, Saalfeld S, Schmid B, Tinevez JY, White DJ, Hartenstein V, Eliceiri K, Tomancak P, Cardona A (2012) Fiji: an open-source platform for biological-image analysis. Nat Methods 9:676–682.

Schueler MG, Sullivan BA (2006) Structural and functional dynamics of human centromeric chromatin. Annu Rev Genomics Hum Genet 7:301–313.

Shaham O, Smith AN, Robinson ML, Taketo MM, Lang RA, Ashery-Padan R (2009) Ashery-Padan R Pax6 is essential for lens fiber cell differentiation. Development 136:2567–2578.

Simmons DD, Tong B, Schrader AD, Hornak AJ (2010) Oncomodulin identifies different hair cell types in the mammalian inner ear. J Comp Neurol 518:3785–3802.

Wang T, Niwa M, Sayyid ZN, Hosseini DK, Pham N, Jones SM, Ricci AJ, Cheng AG (2019) Uncoordinated maturation of developing and regenerating postnatal mammalian vestibular hair cells. PLoS Biol 17:e3000326.

Warchol ME, Massoodnia R, Pujol R, Cox BC, Stone JS (2019) Development of hair cell phenotype and calyx nerve terminals in the neonatal mouse utricle. J Comp Neurol 527:1913–1928.

Wegner M (1999) From head to toes: the multiple facets of Sox proteins. Nucleic Acids Res 27:1409–1420.

Wersall J (1956) Studies on the structure and innervation of the sensory epithelium of the cristae ampullares in the guinea pig; a light and electron microscopic investigation. Acta Otolaryngol Suppl 126:1–85.

Wiwatpanit T, Lorenzen SM, Cantú JA, Foo CZ, Hogan AK, Márquez F, Clancy JC, Schipma MJ, Cheatham MA, Duggan A, García-Añoveros J (2018) Trans-differentiation of outer hair cells into inner hair cells in the absence of INSM1. Nature 563:691–695.

Xiao L, Michalski N, Kronander E, Gjoni E, Genoud C, Knott G, Schneggenburger R (2013) BMP signaling specifies the development of a large and fast CNS synapse. Nat Neurosci 16:856–864.